In situ observations of turbulent ship wakes and their spatiotemporal extent

Amanda T. Nylund[1], Lars Arneborg[2], Anders Tengberg[1], Ulf Mallast[3], Ida-Maja Hassellöv[1]

[1]Department of Mechanics and Maritime Sciences, Chalmers University of Technology, Gothenburg, 412 96 Gothenburg, Sweden.
[2]Swedish Meteorological and Hydrological Institute (SMHI), Gothenburg, 426 71 Västra Frölunda, Sweden.
[3]Department Monitoring and Exploration Technologies, Helmholtz Centre for Environmental Research, Leipzig, 04318 Leipzig, Germany.

Correspondence to: Ida-Maja Hassellöv (ida-maja@chalmers.se)

Abstract. In areas of intensive ship traffic, ships pass every ten minutes. Considering the amount of ship traffic and the predicted increase in global maritime trade, there is a need to consider all type of impacts shipping has on the marine environment. While the awareness about, and efforts to reduce, chemical pollution from ships is increasing, less in known about physical disturbances and ship-induced turbulence has so far been completely neglected. To address the potential importance of ship-induced turbulence on e.g. gas exchange, dispersion of pollutants, and biogeochemical processes, a characterisation of the temporal and spatial scales of the turbulent wake is needed. Currently, field measurements of turbulent wakes of real-size ships are lacking.~~, and t~~This study addresses that gap by using two different methodological approaches: *in situ* and *ex situ* observations. ~~*in situ* and *ex situ* measurements of the depth, width, length, intensity and longevity of the turbulent wake for ~240 ship passages of differently sized ships.~~ For the *in situ* observations, ~~A~~a bottom-mounted Acoustic Doppler Current Profiler (ADCP) was placed at 32 m depth below the ship lane outside Gothenburg harbour.~~,~~ Both the acoustic backscatter from the air bubbles in the wake and the dissipation rate of turbulent kinetic energy ~~and~~ were used to ~~measure~~ quantify the turbulent wake depth, intensity, and temporal longevity for 38 ship passages of differently sized ships. The results from the ADCP measurements show median wake depths of 13 m, and several occasions of wakes reaching depths > 18 m, which is in the same depth range as the seasonal thermocline in the Baltic Sea. The temporal longevity of the observable part of the wakes had a median of around 10 min and several passages of > 20 min. ~~In addition~~In the *ex situ* approach, water temperature was used as a proxy for the water mass effected by the turbulent wake (thermal wake), as lowered temperature in the ship wake indicates vertical mixing in a thermally stratified water column. Thermal satellite images of the Thermal Infrared Sensor (TIRS) onboard Landsat 8 were used to measure thermal wake width and spatial longevity, using satellite scenes from the major shipping lane North of Bornholm, Baltic Sea. Automatic Information System (AIS) records from both the investigated areas were used to identify the ships inducing the wakes. ~~The results from the ADCP measurements show median wake depths of ~10 m, and several occasions of wakes reaching depths > 18 m, which is in the same depth range as the seasonal thermocline in the Baltic Sea. The temporal longevity of the wakes had a median of around 8 min and several passages of > 20 min.~~ The satellite analysis showed a median thermal wake length of 13.7 km (n=144), and the longest wake extended

Commented [AN1]: The changed number is a consequence of the separation of the *in situ* and *ex situ* observations, as well as the revised focus on the close wake category. The additional data (far wakes) has been moved to the supplementary information. In addition, the previous "double wake" category has been omitted completely.

Commented [AN2]: The changed number is a consequence of the separation of the *in situ* and *ex situ* observations, as well as the revised focus on the close wake category. The additional data (far wakes) has been moved to the supplementary information. In addition, the previous "double wake" category has been omitted completely.

over 60 km, which would correspond to a temporal longevity of 1 h 42 min (for a ship speed of 20 knots). The median thermal wake width was 157.5 m. The measurements of the spatial and temporal scales are in line with previous studies, but the maximum turbulent wake depth (30.5 m) is deeper than previously reported. The results from this study, combined with the knowledge of regional high traffic densities, show that ship-induced turbulence occurs at temporal and spatial scales large enough to imply that this process should be considered when estimating environmental impacts from shipping in areas with intense ship traffic. ~~The derived ship induced vertical mixing along with its frequency calls for a better characterisation of spatial and temporal development, given the location of the seasonal thermal stratification of 10–20 m depth and thus the possible impact on local biogeochemical cycles, gas exchange and nutrient distribution.~~

1 Introduction

The shipping industry holds a key role in today's society, as 80–90 % of all global trade is transported via ship (Balcombe et al., 2019). In areas of intensive ship traffic, e.g. in the Baltic Sea, there can be more than 50.000 ship passages annually, which in turn is approximately one ship passage every ten minutes (HELCOM, 2010). Yet, maritime trade is predicted to increase by 3.4 % annually until 2024 (UNCTAD, 2019). Transport by ship is also advocated as the most energy efficient as it in general has low carbon footprint per tonne and distance of transported goods (Balcombe et al., 2019). However, the carbon footprint is only one of many environmental impacts from shipping, and to fully estimate the impact of this growing industry, a holistic assessment is needed (Moldanová et al., 2018). To make a reliable holistic assessment, all types of impacts on the marine environment need to be considered, both from polluting and physical disturbances. This paper will focus on a previously disregarded physical disturbance from shipping, namely ship-induced turbulent wakes and their spatiotemporal extent.

When a ship moves through water, the hull and propeller create turbulence, which forms a turbulent wake behind the ship, characterised by an increased turbulence and an ~~dense~~ intense bubble cloud (NDRC, 1946; Soloviev et al., 2010; Voropayev et al., 2012; Francisco et al., 2017). There are several arguments for the need to ~~K~~know~~ing~~ and be~~ing~~ able to properly characterise temporal and spatial scales of the turbulent wake ~~has several reasons~~. ~~It~~ A characterisation can be used to estimate the distribution of contaminants and pollutants discharged from ships (Katz et al., 2003; Loehr et al., 2006; Golbraikh and Beegle-Krause, 2020). Furthermore, the bubbles created in the turbulent wake can affect the gas exchange between ocean and atmosphere, in addition to the increased gas exchange due to the turbulence itself (Trevorrow et al., 1994; Weber et al., 2005; Emerson and Bushinsky, 2016). The episodic nature, intensity, and duration of the ship-induced turbulence is also of a magnitude that have been shown to affect the mortality of copepods and diatoms (Bickel et al., 2011; Garrison and Tang, 2014). Moreover, in areas with intense ship traffic, the ship-induced vertical mixing could possibly affect nutrient availability and natural biogeochemical cycles in seasonally stratified waters, if the mixing is deep and intense enough to entrain water from below the thermocline.

Commented [AN3]: Revised the use of "it".

Up ~~to~~until now, the environmental impact of ship-induced vertical mixing has been overlooked, and there is a limited amount of field observations reporting spatiotemporal scales of the turbulent wake. There are few studies about ship-induced turbulence in general and none investigating the possible environmental impact of ship-induced vertical mixing. Remote sensing approaches focused on detecting wakes from a surveillance perspective (Fujimura et al., 2016) or the theoretical possibility of doing so (Issa and Daya, 2014). These approaches mainly rely on Synthetic Aperture Radar (SAR) to identify sea surface roughness. Other studies focused on the vertical distribution of the turbulent wake for military purposes, with the interest of detecting the wake and minimizing the wake signal (Smirnov et al., 2005; Liefvendahl and Wikström, 2016). Moreover, the formation and distribution of the bubble cloud in the turbulent wake has been in focus, rather than the turbulence and mixing. Besides the different foci, most of the available studies are numerical modelling studies of ship wakes. Measurements are on model-scale ships for validation (Carrica et al., 1999; Parmhed and Svennberg, 2006; Fu and Wan, 2011; Liefvendahl and Wikström, 2016), which generally only resolve the wake for distances up to a ship length after the ship. In real world, temporal and spatial scales of the turbulent wakes are significantly larger. Turbulent processes are difficult to investigate at laboratory scale, since the Reynolds number is much too small in the laboratory and the results can therefore not be expected to represent turbulence in nature.

The few peer reviewed studies that are based on field measurements or focus on the spatial and temporal scales of the turbulent wake, report measured wake depths between 6–12 m (Table 1). There are also two reports from the grey literature of observed wake depths of 18 m. ~~-~~Measured wake widths are more varied, with a range of 10–250 m (Table 1). This large variation could partly be due to the different methods used to define the wake region, as well as the difference in size and type of the investigated vessel. The longevity of the wake has been measured both as a temporal duration and as a length. Already in 1946, the United States National Defense Research Committee (US NDRC) reported detectable bubbles and temperature differences in the turbulent wake 30–60 min after ship passage. Trevorrow et al. (1994) made measurements of the temporal scale of the turbulent wake and reported strong acoustic scatters from the bubbles in the wake for 7.5 min after passage. Soloviev et al. (2010) evenreported that bubbles from the turbulent wake were visible from 10–30 min after ship passage, corresponding to a distance of 4–10 km, for a ship with a speed of 12 knots. ~~It~~The observations in Table 1 clearly indicate~~becomes clear~~ that the turbulent wake can reach depths of 10–15 m and can have a longevity of up to 30 min and/or 10 km. However, except Trevorrow et al. (1994) and NDRC (1946), information of wake width, length, or duration were always a by-product of these studies. Therefore, they naturally lack simultaneous measurements of depth, width, and length of the turbulent wake, as well as a statistical sound and reliable data basis with a high~~er~~ number and variety of vessels (type, speed, size). Thus, there is currently too few field measurements of the turbulent wake of real-size ships, to reliably estimate the ~~temporospatial~~ spatiotemporal scales of turbulent wakes (Carrica et al., 1999; Parmhed and Svennberg, 2006; Ermakov and Kapustin, 2010).

Commented [AN4]: Revised the use of "it".

The aim of this study is therefore to ~~obtain~~ provide a first ~~reliable~~ comprehensive overview of the magnitude of the spatiotemporal ~~influence~~ extent of ~~ship-induced vertical mixing~~turbulent ship wakes. In order to capture the entire extent of

the turbulent wake, both in all spatial dimensions and time, two different methodological approaches have been used: *in situ* and *ex-situ* observations. ~~through the integration of ~240 observations of ship passages, and a combination of methods to describe the depth, width, length, and longevity of the turbulent wake.~~ As ~~the~~ both ~~study~~ approaches ~~has been conducted *in situ* and *ex-situ*, on different temporal and spatial scales, and~~ include~~s~~ ships of different types and varying size, ~~it~~ the results constitute~~s~~ a solid base for a first estimate of the order of magnitude of the spatiotemporal extent of turbulent ship wakes. A better understanding of the spatial and temporal extent of the turbulent wake, is needed to identify where ship-induced vertical mixing could have a significant impact on local biogeochemical cycles, and thus should be studied further. ~~Moreover, it~~ Knowing the spatiotemporal extent of the turbulent wake also provides a basis for estimating the summed wake area in a region, where an effect on gas exchange could be expected. Finally, knowledge about the turbulent wake extent ~~In addition, it~~ will provide valuable information for monitoring in areas with intense ship traffic, as well as for studies of the dispersion of pollutants from ships. ~~It will be~~The turbulent wake extent is of particular importance for the FerryBox community, as FerryBoxes perform continuous measurements onboard ships en route, often in major ship lanes where mixing from turbulent ship wakes ~~that~~ may lead to biased results compared to surrounding, "natural", water. In short, increased knowledge about the spatiotemporal extent of turbulent ship wakes, makes it possible to identify when and where ship-induced turbulence needs to be considered.

Table 1. Previously reported field measurements of the spatial and temporal scales of the turbulent wake. The method used to estimate the turbulent wake is indicated, as well as the ~~in the "Method" column~~type and number of vessels observed. For studies where only the temporal wake longevity was measured, an estimate of the wake length has been calculated using the wake duration and a ship speed of 12 knots.

Study	Method	Wake depth [m]	Wake length [km]	Wake duration [min]	Wake width [m]	Nr. of Vessels	Vessel type
NDRC (1946)	Acoustic/ thermal	3–10	11–22	30–60	40–90	1–3	Naval, research
Trevorrow et al. (1994)	Acoustic	6–12	2.8*	7.5	66 (avg.)	3	Research
Loehr et al. (2001) ¤	Acoustic	3–18	5–6*	15–17	76–155	2	Cruise ship
US-EPA (2002) ¤	Dye concentration	12–18				4	Cruise ship
Katz et al. (2003)	Dye and paper pulp concentration	8–10	3**			1	Naval
Weber et al. (2005)	Acoustic	8	6	15		1	Research
Stanic et al. (2009)	Acoustic		1.5–2	20	10	1	Research
Ermakov & Kapustin (2010)	Acoustic	4–8	3.7–5.5*	10–15	40–80	1	Small passenger
Soloviev et al. (2010)	Acoustic	10–15	4–10*	10–30		2	Container, cargo
Gilman et al. (2011)	Visible surface trace				100–250	1	Cruise ship
Soloviev et al. (2012)	Acoustic	7				1	Cargo
Francisco et al. (2017)	Acoustic	6–12	0.5*	1.5		2	Passenger ferry

Commented [AN5]: Revised the use of "it".

Commented [AN6]: Revised the use of "it".

Commented [AN7]: Revised the use of "it".

Commented [AN8]: Revised the use of "it".

Commented [AN9]: I have updated this table to add information about the number of investigated vessels and type of vessel, as well as adding two additional reports (non-peer reviewed) to the list of references.

*Calculated based on temporal longevity and a ship speed of 12 knots, **Distance at which the max width was documented, ¤ Grey literature report, not peer reviewed.

2 Materials and methods

To cover all the spatial and temporal scales of the turbulent wake, the data collection was conducted using two different methodological approaches, which focused on ~~The data collection was conducted in two parts~~different aspects of the turbulent wake extent.~~:~~ O~~o~~ne approach was to make *in situ* observations ~~field study~~ in the large ship lane outside Gothenburg harbour, where an Acoustic Doppler Current Profiler (ADCP) was deployed at the sea floor, to observe the vertical scale, the intensity, and the temporal longevity of the turbulent wake (Fig. 1b). The ADCP measurements show the very turbulent core of the wake and provides an estimate of the extent of the turbulent wake. The other approach was based on *ex situ* observations, using ~~and a~~ satellite image analysis of sea surface temperature in the large ship lane north of Bornholm, Baltic Sea (Fig. 1c). ~~. The field study covered the vertical scale and the temporal longevity of the turbulent wake, and the satellite image analysis was used to estimate the~~ T~~t~~hermal wake width and spatial longevity was used as a proxy for the extent of the effect of the turbulent wake. The satellite observations show the thermal signal of the water mass that has been produced by the turbulent mixing during summer conditions, in the form of a wake of colder water trailing the ship's track. The mixed water from the turbulent wake will remain even after the turbulence and bubbles have died away and is a measure of water that has been influenced by mixing. Hence, both approaches provide information for estimating spatial and temporal extent of ship-induced mixing, but the ADCP measurements give an estimate of the turbulent wake, while the satellite image analysis shows the extent of the water influenced by the turbulent wake.

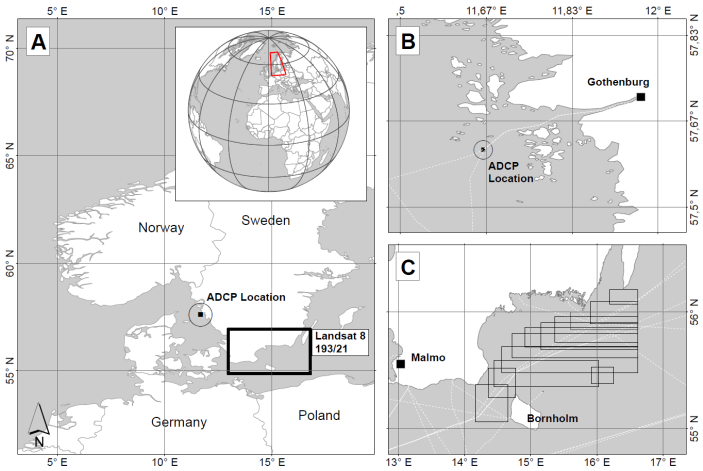

Figure 1: Overview of the two study areas (a) showing the location of the ADCP under the ship lane outside Gothenburg (b) and the area covered by the analysed satellite images (c). White dashed lines indicate ship routes of ferry lines and the boxes in (c) indicate the area defined as the ship lane area in the satellite image analysis. The ship lane and traffic separated zone north of Bornholm are shown in Figure 12.

2.1 Gothenburg harbour study

The field study was conducted off the Swedish west coast, in the large ship lane outside Gothenburg harbour (Fig. 1). Gothenburg harbour is the largest harbour in Scandinavia, with 120 port calls per week, including large container ships, oil tankers, car carriers, and passenger ferries (The Port of Gothenburg, 2020). The size of the harbour, the frequency of port calls, and the variety of ship types, makes it a suitable study area for ship-induced vertical mixing. The site of instrument deployment was outside the port area, under the fairway where all incoming large ships need to pass (Swedish Maritime Administration, 2020). ~~It~~ The site was also inside the area where tugboats and pilots are required when applicable, but outside the speed restriction area, thus ships were traveling at normal speed. For the *in situ* measurements, the Gothenburg site was considered more suitable compared to the Bornholm study area, as ~~it~~ the Gothenburg ship lane was more easily accessible and the risk of losing the instrument to other maritime activities was lower. The water depth at the study site was 32 m, which is similar to the water depth where the major ship lanes on the Swedish West and South coast are located (< 20 m and < 50 m respectively) (Jakobsson et al., 2019). In the Baltic Proper (Western and Eastern Gotland Basins, Northern Baltic Proper), the median depth is deeper (< 75 m), but the major ship lane pass south of Gotland, which is the shallowest part of the Baltic Proper (approximately 25–30 m) (Jakobsson et al., 2019).

Commented [AN10]: Revised use of "it".

2.1.1 Field measurements and data collection

A bottom-mounted Nortek Signature 500 kHz broadband Acoustic Doppler Current Profiler (ADCP) was deployed under the ship lane (57.61178 N, 11.66102 E), fixed in upward-looking position in a bottom frame (Figure 2). Similar setups have previously been used to study the bubble cloud of the turbulent wake by Trevorrow et al. (1994) and Weber et al. (2005). The instrumental setup provides measurements of the overlaying water column trough time (Figure 3), hence, recording the wake development in a fixed point ~~through~~ over time. Under the assumption of a stationary wake moving with the ship velocity, the observations can also be interpreted in terms of the spatial change of the wake with distance from the ship. The instrument was deployed at ~~approximately~~ 32~~0~~ m depth, for a duration of 4 weeks (28 August to 25 September 2018). The ADCP measured along beam current velocities, using four slanted beams (25° angle) and one vertical beam (ping frequency 1 Hz, cell size 1 m on all beams). The echo amplitudes from the beams were also used to detect the wake bubbles. All single ping data on currents and echo amplitude was stored on-board the instruments and analysed, see sect. 2.1.2. The range of sonar frequencies that are suitable for detecting bubbles in the turbulent ship wake is 30 kHz to 1 MHz and depends on the size of the bubbles in the wake (Liefvendahl and Wikström, 2016). A SonTek CastAway®-CTD (Xylem, San Diego, California) was used to measure salinity and temperature profiles at the time of the instrument deployment (August 28, 2018, 4 casts) and retrieval (September 25, 2018, 4 casts).

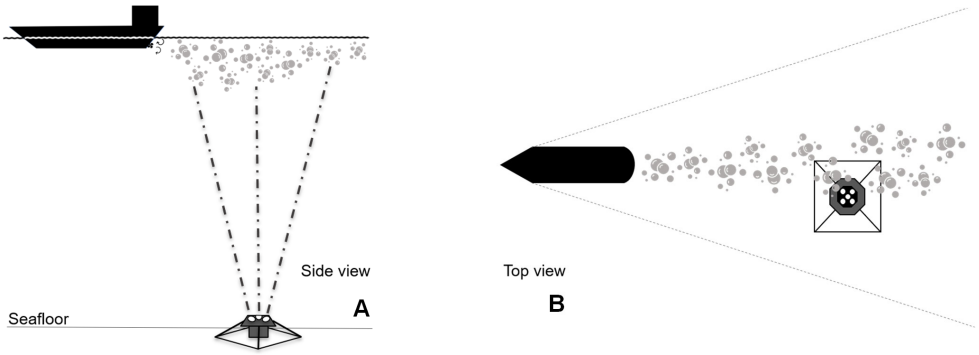

Figure 2: Scheme of instrument deployment, showing a) the sideview with perspective of the ADCP placed on the seafloor facing upward and recording the turbulent wakes during ship passages, and b) a top view perspective of the ADCP recording bubbles from a turbulent wake, induced by a ship passing above, but slightly to the side of the instrument.

A dataset of the ships passing the study area during the field measurement period was purchased from the Swedish Maritime Administration. The dataset is from the Baltic Marine Environment Protection Commission (HELCOM) Automatic Information System (AIS) database, which is processed according to the procedure described in the annex of the HELCOM

Assessment on maritime activities in the Baltic Sea 2018 (HELCOM, 2018). The Swedish Institute for the Marine Environment (SIME) provided additional files from the same HELCOM database, with AIS data for the analysed satellite scenes and the Gothenburg harbour study area. Vessel information from MarineTraffic – Global Ship Tracking Intelligence (www.marinetraffic.com) was used to retrieve detailed information about the width, length and draught of the ships in the dataset.

2.1.2 Data analysis

The data analysis comprised detection and annotation of the turbulent wakes in the ADCP dataset, as well as statistical analysis of the final results. The analysis also included combining the *in situ* observations from the ADCP with the ship tracks and vessel information in the AIS dataset.

Compiling the ADCP wake dataset

All ship wakes in the dataset were identified manually using high resolution figures of the echo amplitude of the ADCP beams (see Fig. 3 for example). As the bubbles in the turbulent wake reflect the sound more efficiently than water, ~~it~~ they induce ~~results in~~ an elevated echo amplitude in the turbulent wake region (NDRC, 1946; Marmorino and Trump, 1996; Trevorrow et al., 1994; Weber et al., 2005; Ermakov and Kapustin, 2010; Francisco et al., 2017). Generally, the wake signal could be clearly distinguished from bubbles induced by waves or signal noise from fish or zooplankton. However, ambiguous cases were noted, mainly during time periods with a lot of waves. ~~and~~ Using a conservative approach,~~the wake dataset was therefore divided into wake categories based on the quality of the wake signal~~ these cases were not considered wakes in the further analysis. Each wake in the dataset was ~~then~~ linked to a ship ~~passing~~track in the HELCOM AIS dataset~~in the vicinity of the ADCP~~, using ~~the HELCOM AIS dataset and~~manual comparison. This introduced additional uncertainties, as not all wakes had clear match with a ship passage. Each ship in the AIS dataset passing within 184 m of the ADCP instrument, was classified either as a **wake inducing passage** or a **no wake passage**. ~~After incorporating the matching uncertainties, the final wake categories used in the analysis were: "~~The wake inducing passages~~",~~ ~~only~~ includ~~ed~~ing all ship passages where a clear wake was detected by the ADCP at the time of ship passage, or after a slight delay (< 15 min). ~~clear wakes with one clear match or delayed match; "double", clear wakes where two or three ships passed the instrument at the same time; and "no wake", which~~ The no wake passages included all passages ~~within 184 m of the instrument that did not induce a~~without a detected wake ~~visible wake~~, as well as all ~~uncertain~~ ambiguous wakes and unclear ship-wake matches~~, which were mostly due to windy conditions which created noisy data.~~ The distance at which a wake can be detected from a passing ship is affected by wake broadening, drifting, and ship width. In this study, the 184 m radius was chosen, as it was the furthest distance at which a clear wake and ship-match was found in the dataset. ~~There were two factors contributing to the existence of the "**double**" category. Firstly, the turbulent wakes in the dataset could be detected from ships passing at distances up to 184 m from the ADCP instrument. Hence, in cases when two ships passed at similar distances from the instrument at the time of a detected wake, it was not possible to distinguish which of the ships induced the wake. Secondly, large ships may require pilot assistance and/or tugboats to enter the harbour.~~

Commented [AN11]: In this section the number of categories has been reduced.

Formatted: Font: Not Bold

Formatted: Font: Not Bold

~~In these cases, the ships pass right next to each other and it is not possible to assign the wake to a single ship.~~ Lastly, some wakes and passages were removed from the analysis altogether. These included ships with missing information in the AIS data (size information), clear wakes where two or three ships passed the instrument at the same time, making it impossible to discern which ship that induced the detected wake, and small ~~sailing vessels~~leisure boats~~, as they due to their small size and engine power were not deemed relevant for the investigated process.~~

Distance calculation, AIS and ADCP dataset

The AIS dataset included position reports for each ship every 2–10 seconds, which were used to calculate the ship's track. The closest distance between the ship-track and the vertical beam of the ADCP instrument was then calculated, using a local planar coordinate system, with the instrument at origo. The coordinates for the closest point on the track was also calculated, using the Python GeoPy package function distance.distance, and the points just before and after the closest point on the track were then identified.

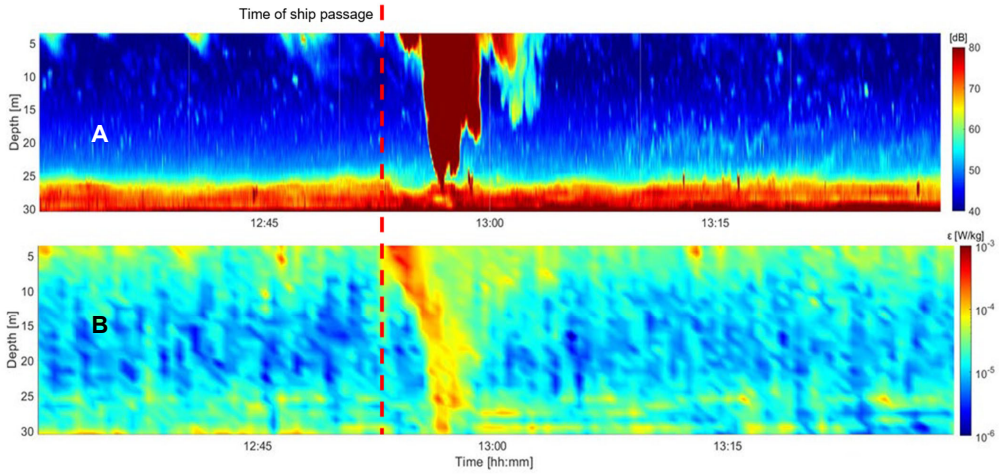

Figure 3: Example of the bubble wake signal in the echo amplitude dataset (a) and the calculated dissipation rate of turbulent kinetic energy, ε, (b) from one hour of ADCP measurements. The upward facing ADCP was placed at ~~approximately~~ 3~~0~~ m depth, repeatedly measuring the water column in one point. The dashed red line marks the time of ship passage. The high intensity red (a) and yellow (b) areas after the ship passage represent the wake region. The increase of ε down to the bottom is evidence of increased turbulence and a vertical mixing down to 30 m depth. The wake was induced by a cargo ship (width 25 m, length 229 m, draught 7 m), which passed the instrument at a distance of 34 m and a speed of 19 knots.

Turbulence calculation, ADCP dataset

The dissipation rate of turbulent kinetic energy (ε) is a measure for the strength of the turbulence. Per definition ε is the rate of energy conversion from kinetic energy to heat due to viscous friction in the smallest eddies, but in a stratified water column ε is also proportional to the mixing between different water masses. There are various ways of determining dissipation rates. In the present work ε is estimated from the ADCP data using the structure function method (e.g. Lucas et al. (2014)), which estimates the dissipation rate of turbulent kinetic energy from the second-order structure function following Eq. (1):

$$D_{11}(r,\Delta r) = \overline{\left(u_r'(r) - u_r'(r+\Delta r)\right)^2}, \quad (1)$$

where u_r' is the fluctuating velocity in the r-direction (in this case the beam direction), Δr is the separation distance between two points along the beam, and overbar denotes time averaging. For separation distances shorter than the largest eddies the structure function relates to the dissipation rate and separation distance as in Eq. (2):

$$D_{11}(r,\Delta r) = C\varepsilon^{2/3}\Delta r^{2/3}, \quad (2)$$

where C is a universal constant. Since the shortest distance (the ADCP bin size) was 1 m, the method is only expected to work for very strong turbulence with vertical eddy scales of magnitude larger than 2–3 m.

For each detected ship wake ~~in the "**wake**" and "**double**" category~~, the along beam current velocity measurements from the ADCP were used for turbulence calculations in the wake region. One of the slanting beams was malfunctioning but the four remaining beams were analysed. A 1-hour dataset following each passage, identified by the start of the bubble cloud, was analysed. Spikes deviating more than four times the standard deviation from the mean in overlapping windows of 100 sec length were removed. Since the velocity signal of surface waves at different depths may be expected to be coherent whereas turbulent signals are not, the two Empirical Orthogonal Function (EOF) modes with largest variance were removed from the series to reduce the influence of surface waves. A fourth order Butterworth high-pass filter with cut-off period 600 sec was used to extract the turbulent velocity fluctuations. The dissipation rate of turbulent kinetic energy was estimated in 30 sec bins using the structure function method according to the method described in Lucas et al. (2014). One dissipation rate estimate was based on the average of the result for the three slanting beams (see Fig. 2 for an example), and another was based on the vertical beam.

Calculating wake depth, longevity, and maximum ε intensity, ADCP dataset

For each detected wake ~~in the categories "**wake**" and "**double**"~~, the wake region was defined for the parameters echo amplitude (bubble wake), dissipation rate of turbulent kinetic energy (ε), and the maximum velocity variance. To reduce noise in the dataset induced by turbidity at the sea floor, the data was normalised with respect to vertical distance from the instrument, assuming exponential decay of the signal strength. The wake region was defined by visual scrutiny of echo amplitude and ε figures (see Fig. 2 for an example) and manually annotated. The elevation in echo amplitude/ε used for delimiting the wake region, as well as the depth and duration to consider, was manually adjusted for each wake to exclude noise. In general, the threshold was ~15% higher compared to the daily/nightly mean. The deepest part of the wake region was used as a measure

of the maximum wake depth and the maximum ε intensity in the wake region was used as a measure of the maximum turbulence. The duration of the wake (temporal longevity in min) was calculated using the start time and end time of the wake region. All calculations were pursued using an individually developed Python code.

Statistical analysis and graphical presentation of the ADCP wake dataset

The statistical analysis was performed for the entire wake dataset (all wakes) and for a subset including ~~For the statistical analysis the categories "**wake**", "**double**", "**close wake**", and "**no wake**" were used. The category "**close wake**", comprises~~ all wakes induced by ships passing within 0–3 ship widths from the instrument (close wakes)~~, which roughly corresponds to 75 m~~. This cut-off was chosen as there was a substantial decrease in the percentage of induced wakes at passages > 3 ship widths from the instrument, indicating difficulties in detecting wakes at larger distances. ~~As the wakes in the "**double**" category lack information about the ship inducing the wake, no "**double**" wakes are included in the "**close wake**" category. Hence the double category is presented separately.~~ For ~~each category~~both all wakes and the close wakes, the median wake depth (m) and temporal wake longevity (min), was calculated for the bubble wake and the ε dissipation rate wake, together with standard deviation (std) and the 25th and 75th percentile. Furthermore, the percentage of ship passages that induced a visible wake in the ADCP beams was calculated along with the maximum ε intensity in the wake region.

For the graphical presentation, the wake depth and longevity results are presented in relation to vessel force (F) [kg m s^{-2}]. F was calculated from the ship width (B) [m], draught (T) [m], and speed (s) [m s^{-1}], as in Eq. (3):

$$F = \rho * B * T * s^2 , \quad (3)$$

with seawater density (ρ) equal to 1025 kg m^{-3}. The F parameter is proportional to ship drag and relates the wake depth and longevity to vessel size and speed, which are parameters affecting the formation of the turbulent wake.

2.2 Bornholm satellite study

The Bornholm study area was chosen, as it covers the most intensely trafficked ship lane in the Baltic Sea, with approximately 50,000 ship passages per year (HELCOM, 2010). All large ships heading for the Eastern and Northern ports of the Baltic Sea, must use the Bornholm ship lane (HELCOM, 2018), which makes it ideal for studying ship-induced vertical mixing from a variety of different ship types. Besides the purely traffic-related reason, ~~a second reason for choosing~~ the Bornholm area was chosen in favour of the Gothenburg area, based on the ~~compared to the Gothenburg area, in which *in-situ* data (ADCP, CTD) was retrieved was the~~ availability of cloud-free satellite scenes~~, which~~. A clear sky is essential for detecting any surface object in the optical and thermal wavelength, and ~~. T~~the Bornholm area (path 193/ row 21) had 23 scenes with less than 23 % cloud cover above the sea until August 2018, compared to ~~for~~ the Gothenburg area (path 196/ row 20) where only 9 scenes were available.

2.2.1 Data collection

All required optical and thermal infrared data from Landsat 8 were retrieved from https://s3-us-west-2.amazonaws.com. The study area for the Bornholm area in the Baltic Sea was covered by path/row 193/21 (see Fig. 1 for overview of study area).

2.2.2 Data analysis

The ships and thermal wakes in the satellite images were detected and annotated using a combination of automatised and manual analysis. The analysis included combining the detected thermal wakes with the ship tracks and vessel information in the AIS dataset, as well as statistical analysis of the results.

Compiling the satellite dataset

To obtain average wake lengths and widths indicating vertical mixing on regional scales, optical, near-infrared and thermal-infrared bands from Landsat 8 were analysed. The dataset includes Landsat 8 data having a cloud cover < 23% (n=23). For optical and infrared data cloud coverage acts as opaque layer hindering to infer any information below it. The procedure includes a general and automatized data pre-processing scheme (Matlab), an automatic ship detection (Matlab) and a manual wake digitization (ArcMap). The pre-processing encompasses i) an automatic download of all available satellite scenes with less than 23% cloud coverage of the given path/row, ii) a masking of land areas using a combination of the modified normalized difference water index (MNDWI) after Xu (2006) and a Otsu-based threshold procedure (Otsu, 1979), iii) a masking of opaque and cirrus clouds classified as such based on the CFMask (Foga et al., 2017), and iv) finally a conversion from top-of-the-atmosphere (TOA) spectral radiances of band 10 to sea surface temperatures (SST) using transmission, downwelling and upwelling radiances modelled for each scene using a MODTRAN based online tool (Barsi et al., 2003).

Detecting ships was pursued semi-automatically following an optical approach similar to the one described by Heiselberg (2016). After masking, the remaining and analysable area is open water only. Spectrally, ships can be differentiated using the visual and short-wave-infrared part of the spectrum, even on the basis of coarser spatial resolution of 30 m as in the present case. As both parts of the spectrum are included in the MNDWI a global threshold of 0.09 was used on the MNDWI image for each scene to detect potential ships. To reduce the number of false positives due to unmasked cloud interference, a further selection criterion was added, using optical ship wake characteristics described in Gilman et al. (2011) and Heiselberg (2016), which is also visible in MDWNI space. Around all potential ships, a search window of 15x15 pixel (450x450m) was created. If MNDWI values > 0.13 representing ship wakes was detected, the potential ship was converted to a true ship, while remaining potential ships were neglected.

Using the ships as spatial indication, all available 23 scenes were screened for thermally indicated ship wakes. In case of an occurrence, all thermal wakes for which a ship was detected, were digitalised. Using this approach, the wake lengths were

obtained (see Fig. 4 for example of visible thermal wakes). To also retrieve wake widths, cross profiles were subsequently created in intervals of 250 m along the thermal ship wake, with a length of 400 m each. The cross-profile lengths were orientated at the maximum widths of < 300 m presented in Gilman et al. (2011). Wake width was automatically determined analysing the local minima (thermal wake centre) and local maxima (surrounding uninfluenced water area) for each of the cross profiles.

Combining the satellite wakes with AIS data

Identified wakes and ships from satellite data were automatically matched against AIS data, to identify the ships inducing the wakes. All scenes were manually controlled to make sure the automatically matched ships were moving in the correct direction to have induced the wake. As the area of interest was the large ship lane north east of Bornholm, only the ships in the traffic separated part of the ship lane stretching from Bornholm to Öland's south tip, were included in the analysis (see boxed area in Fig. 1c). In addition to the matched satellite ships, all other ships present in the area at the time of each satellite scene were identified.

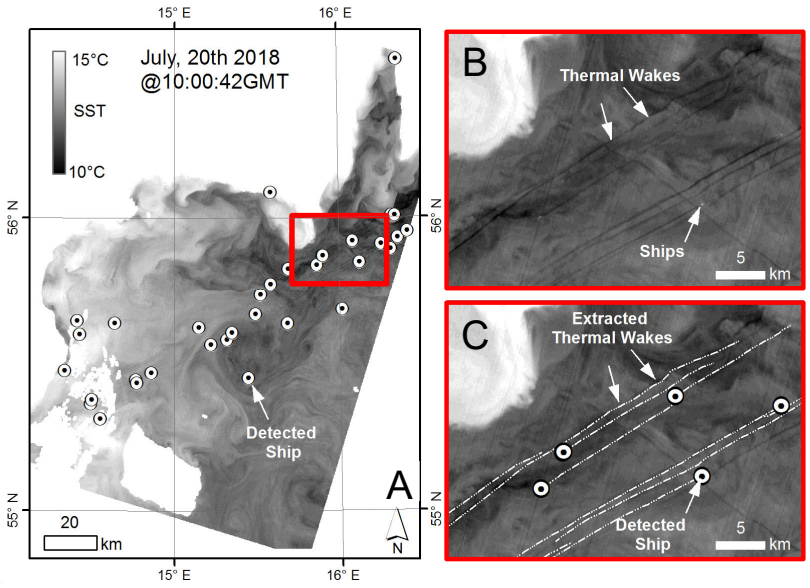

Figure 4: Example of satellite scene with visible thermal wakes in the Bornholm study area, with an illustration of the thermal wake detection process. ~~Note the ships visible as warmer yellow dots and the thermal wakes visible as colder blue lines stretching behind the ships. The oblique regular stripes are not ship wakes, but a sensor induced radiometric artefact.~~(a) is the original satellite scene with the detected ships marked as white circles with black dots. The red box marks the zoomed in area in (b) and (c). In (b), the

thermal wakes are visible as darker lines and the ships as small white dots. (c) shows the detected ships and extracted thermal wakes. **Landsat-8 image courtesy of the U.S. Geological Survey.**

Statistical analysis of satellite wake dataset

For the satellite dataset, the median spatial wake longevity (m) and wake width (m), was calculated, together with standard deviation (std) and the 25th and 75th percentile. The percentage of ship passages inducing visible thermal wakes, was also calculated.

3. Results and discussion

In the Gothenburg harbour study, there was a total of ~~96~~ 68 detected turbulent wakes which could be successfully matched to a passing ship. In the Bornholm satellite image analysis, 144 thermal wakes were detected in the ship lane area, and successfully matched to a ship. Thus, a total of 21~~240~~ ship wakes were included in the analysis, and the results from each study area will be presented separately below.

Commented [AN12]: The double category has been excluded, hence only 68 wakes.

3.1 Gothenburg harbour study

During the measurement period, ~~there were~~ a total of 413 ship ~~passages~~ passed within 184 m of the ADCP instrument, of which 303 were included in the analysis. ~~Of these passages, there were 65 occasions when two ships passed the instrument at the same time. As a double ship passage only induces one wake, these occasions were considered as one passage when looking at the percentage of passages inducing wakes. In addition, 15 other passages were removed due to data uncertainties originating from entirely missing data (n=3), small size vessels irrelevant for the present study such as sailing/pleasure vessels (n=5), and multiple passages or wakes with unclear matches (n=7). This resulted in a total of 333 passages included in the analysis. 96~~ 68 (22 %) of those passages induced clearly visible wakes (all wakes) ~~(29 %) due to single ship passages (n=69) and double passages (n=27),~~ of which 38 (56 %) belonged to the subset. ~~The~~ of close wake passages. ~~(< 3 ship widths from the instrument) comprised 57 % (n=39) of all single ship passages.~~ The close wake passages had a medium passing distance of 29 m and a maximum of 82 m. The ~~statistical analysis of~~ observed wake depth and longevity ~~is presented~~ for the close wakes are presented in section 3.1.4 and 3.1.5, and the results for all wakes are presented in the ~~the entire dataset in section 3.1.4 and 3.1.5~~supplementary information. ~~, together with a graphical presentation of the close wake passage dataset.~~

Commented [AN13]: When both the wake inducing and the non-wake inducing double passages are removed, they sum up to 92.

3.1.1 Environmental parameters

At the time of deployment, there was a clear stratification at 10 m depth, with an upper mixed layer salinity of 25.5, and a gradual increase of salinity below the stratification, reaching a maximum salinity of 32 at 32 m depth (Fig. 54). The temperature profile showed a rather uniform profile, with only a slight increase towards the surface, indicating that salinity was the main stratifying component (Fig. 54). The surface layer had a temperature of 18–18.6 °C, the middle layer ranged from 17.6°C at 10 m to 17.3 °C at 20 m, and the deepest layer went from 17.4 °C to 16.4 at the sea floor. At the time of instrument retrieval,

there was only one clear pycnocline at 5 m depth, with an upper mixed layer temperature around 14 °C and salinity around 27. The temperature below the pycnocline was around 16 °C and the salinity was 33. This type of structure is usual in this area, as the Baltic Surface current which brings low saline water from the Baltic Sea is on top of the more saline water from the Skagerrak (Andersson and Rydberg, 1993) ~~(Snoeijs-Leijonmalm and Andrén, 2017)~~. Note that the water column is unstable in temperature, so also here salinity is the stratifying component.

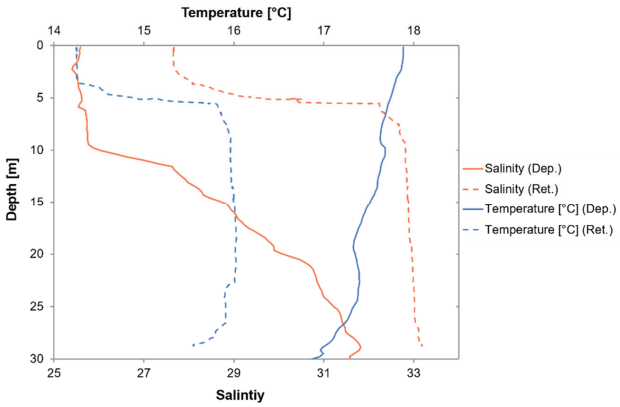

Figure 5: Salinity and temperature at the time of instrument deployment 28 August 2018 (solid lines) and retrieval 25 September 2018 (dashed lines).

3.1.3 Wake detection rate

~~The wake detection rate, related to passing distances and vessel force (F), is show in Figure 6. For passages within 3 ship widths from the instrument (close wake category),~~ For the close wakes subset, the detection rate ranged between 36–100 %, with an average of 5~~6~~7 % (Figure 6). At distances > 3 ship widths, the wake detection was much lower (0–26 %) with an average of 13 %. Due to the low detection rate ~~in the two larger~~at distance~~s categories~~ > 3 ship widths~~, only the close wake category will be used in the graphical presentation of how wake depth and longevity relate to vessel force~~. Surprisingly, the detection rate of wakes induced by ships passing at distances > 3 ship widths does not seem to be affected by the vessel force, as the percentage of detected wakes is similar for all force bins (Figure 6). Similarly, the close wake category does not show a clear correlation between vessel force and wake detection rate. However, more passages with large vessel force would be needed to be able to draw any conclusions regarding the influence of vessel force on wake detection, since the data is skewed towards lower vessel forces. Nevertheless, the results presented in Figure 6, indicates that passing distance affects the wake detection rate more than the vessel force.

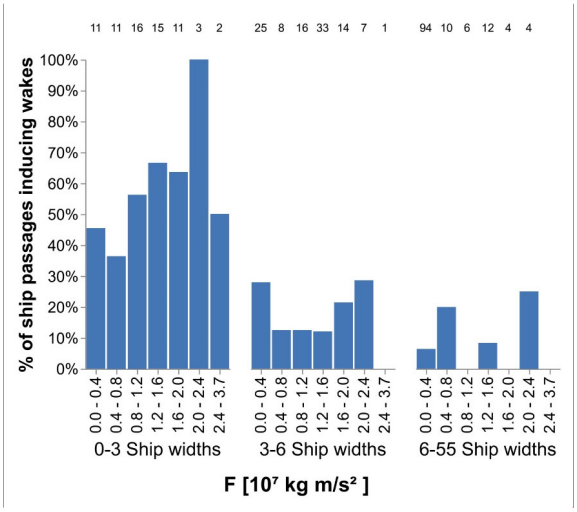

Figure 6. Wake occurrence for three different ~~categories of~~ passing distances: 0–3, 3–6, and 6–55 ship widths from the instrument. For each distance ~~category~~, the x-axis shows the force (F) of the passing vessel in Newton. The number above each bar indicate the total number of passages for that ~~category~~passing distance. Note the cut-off in percentage detected wakes at passing distances > 3 ship widths.

3.1.4 Maximum wake depth

The median maximum wake depth for ~~for all~~the close wakes was 11.5 m (std 4.3 m) ~~9.5 m (std 4.2 m)~~ for the bubble wake and 13.5 m (std 3.7 m)~~11.5 m (std 3.9 m)~~ for the ε wake (Table 2). ~~The close wake category had larger median values for both the bubble wake and ε wake, at 11.5 m (std 4.3 m) for the bubble and 13.5 m (std 3.7 m), respectively.~~ These ε wake depths were not the lower weak rim of the wake, as the threshold values defining the wake region mostly ranged between 10^{-4}–$10^{-3.5}$ W kg^{-1}. These threshold values are ~~really~~ large (e.g. Thorpe (2007)), indicating vigorously turbulent wakes, which probably were homogeneous down to the maximum depths of the wake region. Previous peer-reviewed studies have mainly reported turbulent wake depths of 8–12 m, with two observations from the grey literature of wake depths of 18 m (Table 1). ~~In contrast, the results from this study show that 25 % of the detected bubble wakes were deeper than 12.5 m and 25 % of the ε wakes were deeper than 14.5 m (Table 2).~~ The deepest detected wakes reached values of 27.5 m for the bubble wakes and 30.5 m for the ε wake. These maximum values are > 10 m deeper than previously reported ~~maximum~~ depths in the grey literature and > 15 m deeper than previously reported in peer reviewed studies (Table 1). The wakes detected from ships passing > 3 ship widths from the instrument does not give a full representation of the maximum wake depth or longevity, as they likely represent the outer edges of the wake region. Nevertheless, these observations still provide information about the wake depth 3–55 ship widths from the

Commented [AN14]: Unit on figure axis has been updated.

wake centre (30–180 m), and the observe median values were 7.5 m and 9.5 m for the bubble wakes and ε wakes respectively (Supplementary info, Table 1).

Table 2. Mean, median, maximum value, first quartile (Q25), third quartile (Q75), and standard deviation (std), for wake depth and longevity, for the observed ~~the wake categories~~wakes induced by ships passing ~~; close wakes (~~0–3 ship widths~~)~~ from the ADCP instrument~~.~~, single wakes, double wakes, and all wakes in the dataset.

Bubble wake depth [m]						Bubble wake longevity [min]					
Mean	Median	Max	Q25	Q75	Std	Mean	Median	Max	Q25	Q75	Std
11.8	11.5	27.5	9.5	13.5	4.3	00:11:00	00:09:59	00:28:59	00:06:29	00:13:15	00:06:34
~~10.3~~	~~9.5~~	~~27.5~~	~~7.5~~	~~12.5~~	~~4.1~~	~~00:10:14~~	~~00:08:00~~	~~00:28:59~~	~~00:05:29~~	~~00:13:29~~	~~00:06:29~~
~~11.2~~	~~10.5~~	~~22.5~~	~~8.5~~	~~13.5~~	~~4.4~~	~~00:12:21~~	~~00:11:29~~	~~00:23:29~~	~~00:07:00~~	~~00:19:00~~	~~00:06:23~~
~~10.6~~	~~9.5~~	~~27.5~~	~~7.5~~	~~12.5~~	~~4.2~~	~~00:10:50~~	~~00:08:44~~	~~00:28:59~~	~~00:05:53~~	~~00:15:45~~	~~00:06:29~~

~~ε~~ wake depth [m]						ε wake longevity [min]					
Mean	Median	Max	Q25	Q75	Std	Mean	Median	Max	Q25	Q75	Std
13.4	13.5	30.5	11.5	14.5	3.7	00:06:17	00:05:59	00:13:30	00:04:45	00:07:44	00:02:33
~~11.8~~	~~11.5~~	~~30.5~~	~~9.5~~	~~13.5~~	~~3.9~~	~~00:06:22~~	~~00:05:59~~	~~00:13:59~~	~~00:04:59~~	~~00:07:59~~	~~00:02:41~~
~~12.9~~	~~11.5~~	~~19.5~~	~~9.5~~	~~17.0~~	~~3.8~~	~~00:09:07~~	~~00:08:00~~	~~00:20:00~~	~~00:06:44~~	~~00:10:14~~	~~00:03:53~~
~~12.1~~	~~11.5~~	~~30.5~~	~~9.5~~	~~14.5~~	~~3.9~~	~~00:07:08~~	~~00:06:30~~	~~00:20:00~~	~~00:05:00~~	~~00:08:30~~	~~00:03:18~~

Distance to instrument [m]						
Mean	Median	Max	Q25	Q75	Std	n
32	29	82	16	42	21	3~~89~~
~~64~~	~~46~~	~~184~~	~~26~~	~~101~~	~~51~~	~~69~~
~~31~~	~~18~~	~~120~~	~~9~~	~~46~~	~~32~~	~~27~~
~~55~~	~~38~~	~~184~~	~~16~~	~~82~~	~~49~~	~~96~~

In Figure 7, the maximum wake depth is presented for the bubble wake and ε wake, in relation to vessel force (F). For the bubble wake, the percentage of induced wakes deeper than 12 m increases with increased vessel force~~, which can be seen in both the close wake category~~ (Fig. 7a) ~~and all single wake passages (Fig. 7b)~~ and~~.~~ ~~T~~There ~~is~~ was a similar tendency for the ε wake~~, although the tendency is more prominent in the figure of all single wake passages~~ (Fig. 7b~~d~~). However, there was no statistically significant correlation between F and maximum wake depth for either category. The lack of correlation could partly be explained by the skewed data distribution, as there were few passages with a large F (Figure 6).

Comparing the median maximum wake depth for the bubble wake and the ε wake~~, for the entire dataset,~~ the ε wake was slightly deeper ~~for all categories~~ (~~~~12~~ m) (Table 2, Fig. 7). The bubbles in the wake are an indication ~~that~~ of surface water ~~has~~ be~~e~~ing mixed down at depth and that it has been mixed with the ambient water. The bubbles will remain in the water column, or they can rise or collapse with time, depending on the bubble size. Bubbles with positive buoyancy will have an upward motion counteracting the downward mixing, which could be one explanation to why the bubble wakes are slightly shallower than the ε wakes. The dissipation rate of turbulent kinetic energy on the other hand, is a measure of the turbulent motions in

Formatted Table

Commented [AN15]: Table has been revised to only include the close wake subset.

the water that mixes the water down. When the turbulence decays, the dissipation also decays and dies out. ~~As t~~The bubbles may remain after the turbulence has died out, ~~it~~ which can explain why the bubble wake lasts longer compared to the ε wake. Another possible explanation to why the ε wakes are deeper is the calculation method used. The dissipation estimate is influenced by neighbouring cells (Eq. 1) and if there is strong turbulence in one cell and none in the next, the method may still show some turbulence in the calm cell.

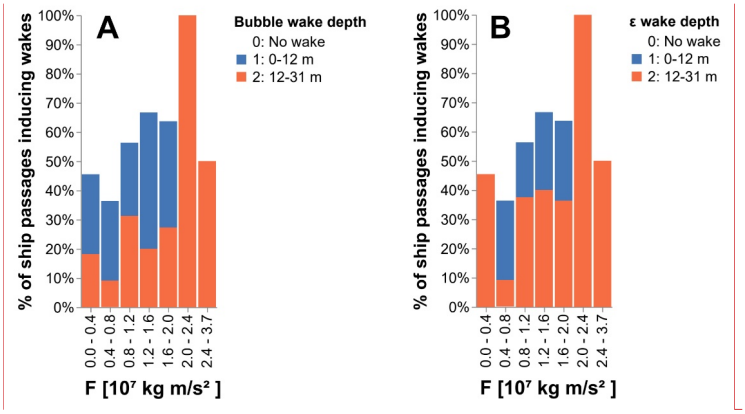

Commented [AN16]: Unit on figure axis has been updated.

Figure 7. Maximum wake depth for the bubble wake (a~~, b~~) and dissipation rate of turbulent kinetic energy (ε) wake (b~~c, d~~)~~. (a) and (c) are show~~ for ~~the close~~detected wakes~~,~~ induced by ships passing at 0–3 ship widths from the instrument~~,~~ ~~and (b) and (d) show all wakes induced by single ship passages.~~ The x-axis shows the force (F) of the vessel in Newton. Wake depths within the range presented in previous peer reviewed studies are shown in blue and wakes deeper than previously reported are shown in orange.

Among the ADCP measurements, there were a few wakes which reached depths of >18 m (Table 2). The deepest wake, >30 m, observed in this dataset was induced by a cargo ship with a beam of 25 m, length of 229 m, and draught of 7 m. The ship passed the instrument at a distance of 34 m and a speed of 19 knots. The cargo ship had a Gross Tonnage similar to the average of container and Ro-Ro cargo ships in the Baltic Sea (HELCOM, 2018), indicating that ship-induced mixing to depths of 30 m could be a common, but undetected occurrence. The hypothesis that vertical mixing to this depth could be more frequent than expected from previous studies (Table 2) is supported by the observations that similarly sized ships passing at the same distance as the cargo ship inducing the deepest wake, also induced mixing to depths greater than 15 m. On the other hand, the difference in wake depth for ships of similar size and passing distance could also be due to differences in stratification, as a strong stratification can dampen the vertical development of the wake (Kato and Phillips, 1969). During the ADCP measurement campaign, water column stratification was measured at deployment and retrieval of the instrument (Fig. 4). Three hours before the instrument retrieval, a cargo ship passed at a distance of 21 m and induced a bubble wake of 13.5 m depth and a ε wake 17.5 m depth. At the point of retrieval, CTD measurement showed a strong thermal stratification at 5 m depth.

At the time of ship passage, intense vertical mixing induced the wake down to 17.5 m depth, and the likelihood that the thermal stratification at 5 m depth was intact during the longevity of the wake, is small. This means that the stratification was strongly influenced by the wake and that waters above and below the thermocline were mixed with each other. Three hours later the water had re-stratified and the mixed water had spread out laterally, but the effect of the mixing, in terms of changes of the physical and chemical characteristics of the water mass, is irreversible. However, the effects of the mixing event that remain after re-stratification (i.e. changes in chemical composition, gas exchange, temperature), are not possible to observe with the methods used in this study. Still, ship-induced turbulence interacts with the local and regional stratification, even though the contribution from each single ship is difficult to observe after the water has re-stratified. The lack of previous reports of vertical mixing of this magnitude can partly be explained by the fact that no previous study has targeted this specific research question. Moreover, measurements made using similar methods, but for other purposes, are seldom conducted in ship lanes and particularly not from below. Further studies are needed to determine the interaction between a stratification and the vertical development of the turbulent wake, and the importance of the ship's draught and speed. The results from this study show that vertical mixing to depths down to 30 m occurs, and possibly at a high frequency, but the current knowledge about the wake distribution is poor (especially on a vertical scale), and further studies are needed to determine when, and at what frequency, vertical mixing reaching this depth occurs.

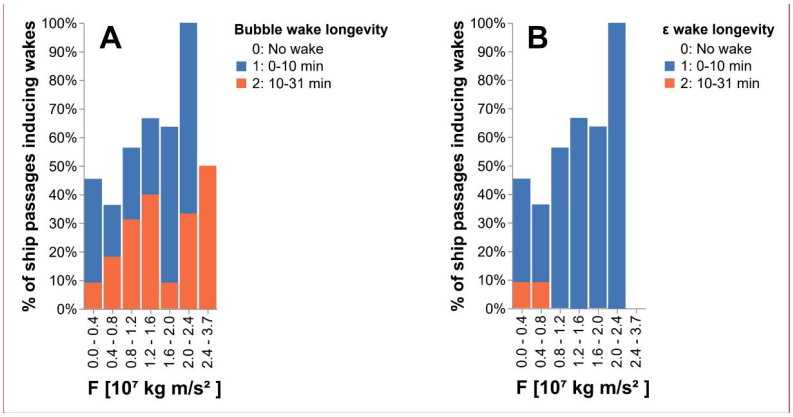

Figure 8. Wake longevity for the bubble wake (a~~, b~~) and dissipation rate of turbulent kinetic energy (ε) wake (b~~e~~, d~~)~~). ~~(a) and (c) are show the close~~for detected wakes~~, induced by ships passing at 0–3 ship widths from the instrument~~. ~~, and (b) and (d) show all wakes induced by single ship passages.~~ The x-axis shows the force (F) of the vessel in Newton. Wake temporal longevities < 10 min are shown in blue and wake longevities 10–31 min are shown in orange.

3.1.5 Temporal wake longevity

Figure 8 shows the wake temporal longevity related to vessel force, for ~~the same wake categories and parameters as in Figure 7~~the bubble wake and ε wake. The median longevity ~~for all wakes~~ was 09:59 min (std 06:34 min) ~~08:44 min (std 06:29)~~ and

Commented [AN17]: This paragraph has been moved from section 3.4.

Commented [AN18]: Unit on figure axis has been updated.

0~~5~~6:~~59~~30 min (std 0~~2~~3:~~33~~18~~)~~) for the bubble and ε wake respectively~~)~~ (Table 2).~~ The close wake category had the same longevity for the ϵ wake, but the bubble wake was longer at 09:59 min (std 06:34 min).~~ Figure 8 shows no clear correlation between wake longevity and vessel force, for the bubble or ϵ wake. Hence, the results from this study, indicate that parameters related to the vessel speed and size do not explain the variation in wake longevity to a very high degree. However, the relatively low number of passages with a large vessel force makes it difficult to draw any definite conclusions without further studies.

~~In similarity with the maximum wake depth, the double category had a longer duration on average, compared to the single categories, for both the bubble and ϵ wakes (Table 2). A majority of the longest wakes (20–30 min) were induced by ships passing within 3 ship widths of the instrument (Fig. 8). As this indicates that proximity plays a role in the ability to detect the entire temporal longevity of the wake, the close wake category median would be a better estimate of wake longevity, compared to the median longevity calculated from all detected wakes. Compared with previous studies, a~~ A detectable signal of the bubble wake from 10 and up to 30 min, is in agreement with previous studies (Table 1). Furthermore, the timescale of the wake longevity indicates that in highly trafficked areas, where large ships passes every 10–15 min, there is a high potential of a constant influence of ship-induced vertical mixing.

3.2 Bornholm satellite image analysis

There was a total of 94 satellite scenes from the period April 2013 to December 2018. Of these scenes, 25 % had a cloud cover of < 23 %, and were analysed for thermal wakes. 48 % of these (n=11) had visible thermal wakes. The monthly distribution of ship passages and occurrence of thermal wakes are shown in Figure 9. As the number of analysed satellite scenes differed between months, the total number of ship passages for each month was divided by the number of analysed scenes. For all months, the majority of the passages did not induce visible thermal wakes. In April-July, there were several induced thermal wakes per scenes (Fig. 9), most of them in May and June. Occasional thermal wakes were found in September and October, but none were found during the winter months (December–February). In the satellite scenes where thermal wakes were visible, and the environmental conditions were right for thermal wakes to be visible, 21 % of the ship passages induced thermal wakes (Table 3). ~~Looking at~~For all the satellite scenes, including those without environmental conditions appropriate for inducing visible thermal wakes, 10 % of the ship passages induced thermal wakes.

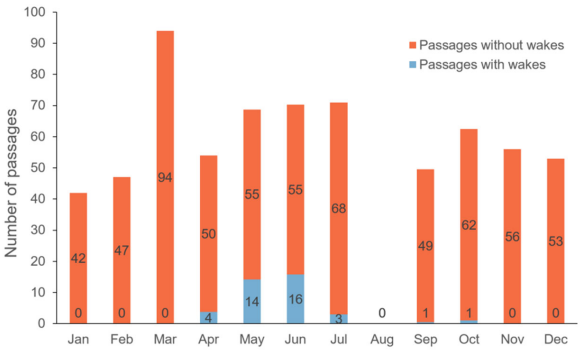

Figure 9. Seasonal distribution of ship passages for the satellite scenes with < 23 % cloud cover, for the period April 2013 to December 2018. The data labels in the stacked bar indicate the number of passages in each category. As some month has more than one analysed scene, the total number of ship passages for each month was divided by the number of analysed scenes, to get an average number of passages per scene for each month. August had no scenes with < 23 % cloud cover and therefore has no data.

Table 3. Number of ship passages in the analysed satellite scenes and the percentage of passages inducing thermal wakes.

	Number of passages	% induced thermal wakes
Total passages	1430	10%
Total passages in scenes with thermal wakes	684	21%
Matched thermal wakes	144	
Unmatched thermal wakes	9	

3.2.1 Spatial wake longevity

The median length of the matched thermal wakes in the ship lane area was 13.7 km (std 11.8 km), and 25 % were ≥ 20.9 km (Fig. 10a). Assuming that the median speed of the wake-inducing ships in the dataset (13.0 knots) is representative for the ship speed in the area, the calculated temporal wake longevity for the median wake length of 13.7 km was 34 min. The longest thermal wake was 62.5 km, which considering the speed of the wake-inducing ship (20 knots), corresponds to a longevity of 1 h 42 min. In model experiments by Voropayev et al. (2012), the thermal wake signature was still increasing at a distance of 30 ship lengths behind the ship, which would correspond to 6 km for a 200 m long ship. Thus, the thermal wake length reported in the current study, are up to one order of magnitude larger than previously reported experimental results, indicating an underestimation of thermal wake longevity in previous studies.

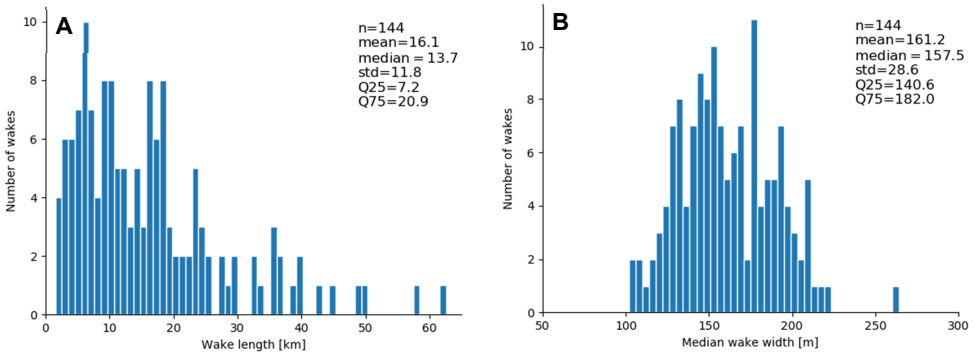

Figure 10. Distribution of observed thermal wake ~~Wake~~ length~~s~~ (~~left~~a) and ~~mean~~ width~~s~~ (b), ~~of thermal wakes~~ in the ship lane area indicated in **Figure 1**c. The observations are from~~,~~ ~~in~~ satellite scenes with visible thermal wakes and < 23 % cloud cover, for the period April 2013 to December 2018 (n=144).

3.2.2 Spatial wake width

The thermal wake width distribution is presented in Figure 10b and Figure 11. The median wake width for the entire dataset was 157.5 m (std 28.6), which is within the ~~range~~ 10–250 m range presented in previous studies (Table 1). There was no correlation between vessel width, length or force [N], versus thermal ship wake width or length (data not shown). The width in this study corresponds to the values presented in Gilman et al. (2011), who ~~also~~ used a ship-based remote sensing approach to estimate width from the visible wake on the sea surface. In contrast, Trevorrow et al. (1994) and Ermakov and Kapustin (2010) reported typical widths of 40–80 m, which is narrower than any widths detected in the current study. However, the last two studies used acoustic measurements of bubbles to estimate the wake width, which could explain the diverging results. The distribution of the median wake width for the different satellite scenes can be seen in Figure 11. Variations in stratification conditions could be one of the explanations to why the thermal wake width varied between scenes. Another reason could be local and regional wind conditions as pointed out in Gilman et al. (2011), or simply the varying temperature gradient between entrained cooler temperatures and warmer temperatures of the upper layer and the resulting exponential adaption process given Newton's law of cooling (Vollmer, 2009; Mallast and Siebert, 2019).

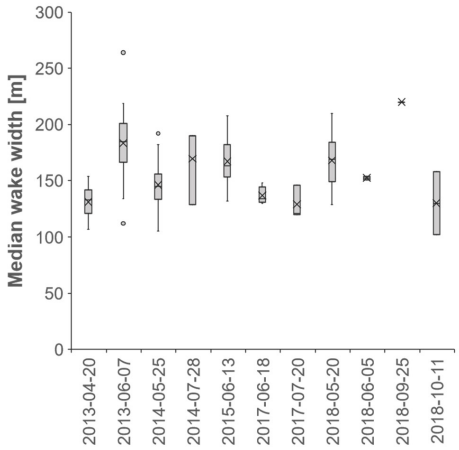

Figure 11. Median wake width distribution for the thermal wakes in the 11 satellite scenes with visible thermal wakes and < 23 % cloud cover, for the period April 2013 to December 2018. The median values are indicated with an X and outliers with rings (o).

3.3 Possible environmental ~~I~~implications ~~of the spatial and temporal scales~~ of turbulent wakes

~~T~~To put the effect of turbulent wakes at the observed spatiotemporal scales in the context of possible environmental implications, an example from the Bornholm area can be used. The traffic separated ship lane in the sound north of Bornholm is intensely trafficked, with 50,000 ship passages every year (HELCOM, 2010). Zooming into the shipping lane area and the traffic separation zones (each 5 km wide and ca 30 km long), there is typical 4-5 ships present in each direction, at any given time (Figure 12). ~~he environmental implications of the spatiotemporal scales of the turbulent wake presented in this study can be illustrated by an example.~~ Using the longevity and width of the "median" ~~turbulent~~ thermal wake as a proxy for the effect of the turbulent wake, ~~it is possible to estimate~~ the area of the shipping lane being affected by the turbulent wake, at any given time, can be estimated. Considering a scenario where all four wakes are uniformly distributed without overlap~~, four wakes in total~~ (Figure 12). ~~The traffic separated ship lane in the sound north of Bornholm is intensely trafficked, with 50,000 ship passages every year (HELCOM, 2010). A typical example of the number of ships present in the area at any given time can be seen in Figure 12~~Figure 12, which shows the ships with AIS transmitters present in the sound at the time of the satellite scene ~~from 2014-05-25 10:01. The ship lane area and the traffic separation zone are indicated, with each ship lane being 5 km wide and approximately 30 km long, which correspond to an area of 150 km^2. During the time of the satellite passage, there were four ships present in both the south-east ship lane in the traffic separated part in the Bornholm sound, and in the north-west ship lane. The~~a median thermal wake length ~~of (~~13.7 km~~)~~ and width of ~~(~~157.5 m~~)~~ (Fig. 9), the ~~gives an average~~ thermal wake area ~~of is~~would be ~~2.16 km^2. Consider a scenario where all wakes are uniformly distributed without overlap. With no overlapping wakes, four median ship wakes would cover an area of~~ 8.6 km^2~~. With a ship lane area of 150 km^2, the area covered~~

~~by thermal wakes would correspond to~~, i.e. 5.8 % of the ship~~p~~ping lane. ~~Considering~~ However, considering the frequent ship traffic in the Bornholm sound ~~and the satellite observations in this study~~, the presence of eight ships in each separation zone at the same time should occur frequently~~. In this case the covered area would be 17.3 km^2~~, ~~which corresponds to~~implying 11.5 % thermal wake coverage.

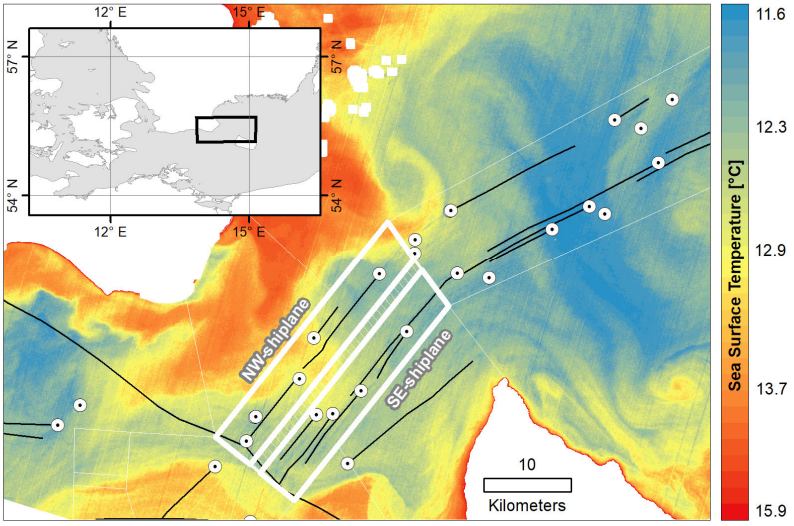

Figure 12. Ships and visible thermal wakes in the Bornholm sound from the analysed satellite scene from 2014-05-25 10:01. White circles with black dots indicate ships with an AIS transmitter present in the area at the time of the satellite passage, and the black lines are the digitalised visible thermal wakes from the satellite scene. White lines indicate the ship lane area, the bold lines mark the North-West and South-East ship lanes, and the dashed area is the traffic separation zone. Landsat-8 image courtesy of the U.S. Geological Survey.

In addition to ~~an~~ the estimate of the area affected by the turbulent wake through its thermal signature, it is also possible to consider the frequency at which the water mass in a certain point would be influenced by a turbulent wake. An average of 50,000 ship passages in the Bornholm sound, corresponds to 25,000 passages in each direction, ~~which divided over a year would~~ corresponding to approximately one passage every 21 min (~ 3 per hour). Considering a scenario~~,~~ where ~~instead of a uniform distribution of ships in the entire ship lane,~~ all ships travel along the exact same path. The calculated median temporal thermal wake longevity for the satellite data was 34:00 min. As the thermal wake longevity is longer than the average time between ship passages, the assumption that all ships travel the exact same route would mean that the water mass along the travelled route would be under constant influence of a ship-induced thermal wake. ~~Now consider t~~The same scenario~~, but~~ can also be ~~using~~ assessed using the median temporal longevity for all the ADCP wake measurements from the close wake

passages, 09:59 min for the bubble wake and 05:59 min for the ϵ wake (Table 2). ~~As the bubbles in the turbulent wake are visible for 09:59 min, t~~The assumption that there is a ship passage every 21 min means that there is 11min between each ship passages when there are no bubbles, i.e. the shipping lane will be influenced close to 50% of the time. If using the median temporal longevity for the ϵ wake instead, the shipping lane would be influenced close to 30 % of the time (~~would be~~ 15 min intervals without turbulence). ~~In~~ Figure 12~~Figure 12, some of the wake tracks are overlapping, thus it does not fully correspond to the scenario of uniformly distributed wakes. However, the figure still gives a conceptual visualisation of how large the part of the ship lane area is that can be influenced by thermal wakes.~~

~~Hence, the bubble wake would influence the water mass in a certain point every 11 min and the ϵ wake every 15 min~~~~The difference in temporal longevity, between the ADCP measurements and satellite observations, can partly be explained by the fact that the two methods measures different aspects of the turbulent wake.~~ ~~The ADCP measurements show the very turbulent core of the wake. The dissipation rate of turbulent kinetic energy (ϵ) gives an estimate of the intensity of the mixing, and both the ϵ and bubble wake gives an estimate of the spatial scales of the turbulent wake. The satellite observations, on the other hand, show the thermal signal of the water mass that has been produced by the turbulent mixing. The mixed water from the turbulent wake will remain even after the turbulence has died away, and is a measure of water that has been influenced by mixing. Hence, both methods can be used to estimate the spatial and temporal scales of ship-induced mixing, but the ADCP measurements give an estimate of the turbulent wake, and the satellite analysis shows the scales of the water influenced by the turbulent wake.~~

The above calculated area coverage of thermal wakes, and the frequency at which the water mass in a certain point would be influenced by ship-induced mixing, represents two extremes. The first scenario assumes a uniform distribution of all ship wakes, and the second scenario assumes that all ships travel along the same route. However, in reality some of the wake regions would be overlapping (e.g. see Figure 12), and most ships would travel similar, but slightly different routes in the ship lane. Nevertheless, based on the results presented in this study, areas like the Bornholm ship lane in the Baltic Sea could be considered under a near constant influence from ship-induced turbulent mixing. Even if the water column regains its stratification quite quickly, the mixing of the wake water with the surrounding water would take much longer (Arneborg, 2002). In a natural marine system, the water column is often stratified due to surface heating and/or freshwater influence. The wake turbulence interacts with this stratification by mixing the water and entraining deeper waters into the wake. The stratification may, in turn, reduce the vertical extent of the wake relative to what it would have been in a homogeneous water column (e.g. Voropayev et al. (2012)). During periods of seasonal stratification, nutrients in the surface layer are depleted, and the supply of nutrients from below is limited due to damping of the vertical mixing by the stratification (Reissmann et al., 2009; Snoeijs-Leijonmalm and Andrén, 2017). In coastal regions, nutrients can be brought up to the upper mixed layer by coastal upwelling, but in ~~the~~ open ~~ocean~~water, the nutrient supply is dependent on vertical mixing (Reissmann et al., 2009). If the vertical mixing is intense and deep enough, ~~it~~ the mixing will bring up nutrient rich water from below the stratification to

the upper surface layer, which can increase primary production and sustain algal blooms. In ocean systems unaffected by human activities, vertical mixing in the surface layer is induced by wind, and the depth of the mixing depends on the wind strength and duration, as well as the input of buoyancy from heating and fresh water (Thorpe, 2007). In temperate oceans like the Baltic Sea, the seasonal thermal stratification ~~occurs during the summer season~~, at 10–20 m depth (Stigebrandt, 2001; Leppäranta and Myrberg, 2009), occurs during the summer season, which is also the period with the least wind (Reissmann et al., 2009). Thus, in unaffected seasonally stratified waters, there is little vertical mixing during the summer months. However, in areas with intense ship traffic there is a frequent input of ship-induced vertical mixing. In the Baltic Sea, at any given moment, there are circa 2000 moving vessels (HELCOM, 2010). A scoping calculation based on the average main engine power and velocity per ship type presented in Jalkanen et al. (2014), and the distance travelled by each ship type from Hassellöv et al. (2019), will give a yearly input of turbulent kinetic energy from ship wakes of 3.9 GW. Using the conservative assumptions 1) that ~~Based on the total surface area of the Baltic Sea (including Kattegat and Skagerrak) and using the conservative assumption that~~ the ships are running at ~~50~~ 50 % Maximum Continuous Rating (MCR) (Buhaug et al., 2009; Smith et al., 2015), and 2) that the ships are operating evenly distributed on the total surface area of the Baltic Sea (including Kattegat and Skagerrak), the average energy input from turbulent ship wakes would be 0.0044 W m^{-2}. This ship-induced turbulent kinetic energy will mostly dissipate, but a certain fraction will be used to mix the water column in case of stratified water. This ~~is to~~can be compared with the dissipation rate of turbulent kinetic energy caused by wind and wave generated turbulence. Below the direct wave breaking layer, about one wave height thick (e.g. Sutherland and Melville (2015)), the dissipation rate of turbulent kinetic energy follows the "law of the wall" (Thorpe, 2007). There, the integrated dissipation rate of turbulent kinetic energy between the depths z_1 and z_2 can be written as Eq. (4):

$$\rho_0 \frac{u_*^3}{\kappa} ln \frac{z_2}{z_1} \quad (4)$$

where ρ_0 is the water density, κ is the von Kármán constant (≅ 0.4), and u_* is the friction velocity. The friction velocity can be estimated from the wind velocity at 10 m height (U_{10}) as Eq. (5):

$$u_* = \sqrt{\frac{\rho_a}{\rho_0} C_D U_{10}} \quad (5)$$

where ρ_a is the air density, and C_D is a drag coefficient. An estimate of the integrated wind generated dissipation rate at Gotska Sandön in the Baltic Sea between 1 and 20 m depth gives 0.002 W m^{-2} in summer time and 0.007 W m^{-2} in wintertime, based on wind observations and using the parameterization of Smith (1988) for the drag coefficient. The dissipation rate of turbulent kinetic energy caused by vessels is therefore double the size of ~~one order of magnitude larger than~~ that caused by winds during summer at the depths where the turbulence may cause mixing of the seasonal thermocline. That is when averaged over the whole basin. The local impact in shipping lanes and behind individual ships is much larger. ~~In t~~The Baltic Sea~~, the~~ seasonal thermal stratification is located at 10–20 m depth (Stigebrandt, 2001; Leppäranta and Myrberg, 2009), and in many of the areas where the major ship lanes are situated, the median water depth is between 20–50 m (Jakobsson et al., 2019). Consequently,

during summer stratification, ship-induced turbulent mixing has a large potential to alter ~~gas exchange and~~ nutrient availability and gas exchange on a local/regional scale, which should be considered when evaluating environmental impact from shipping.

The results presented in this study, also have implications for monitoring and data collection in areas with ship traffic~~; . An especially interesting example are the so called~~particularly when using FerryBox systems~~, which are placed on ships and~~ to conduct automated continuous measurements of parameters such as O_2 concentration, salinity, temperature, and sometimes also pCO_2, Chlorophyll a, and pigments (Petersen, 2014). In the Baltic Sea t~~T~~here are currently seven passenger ferries equipped with FerryBox systems ~~in the Baltic Sea, which are,~~ traveling along the major shipping lanes all or part of the journey (https://www.ferrybox.com/routes_data/routes/baltic_sea/index.php.en). The intake of water to the FerryBox is from an inlet in the ship hull, ~~corresponding to~~located at approximately 2–10 m depth (Petersen, 2014)~~, which would correspond to somewhere between 2–10 m depth~~. Considering the wake longevity of the thermal and turbulent wake observations~~s~~ presented in this study, there is a high likelihood that a ship traveling in a major ship lane, could be moving in the wake of another ship. In that case, the water being ~~measured~~ analysed by the FerryBox is the water of the turbulent wake, and thus not necessarily representative for the conditions outside the shipping lane. Karlson et al. (2016) performed v~~The v~~alidations ~~made for~~of FerryBox data, which was in good agreement with data from discrete water sampling in the shipping lane. ~~measurements are being made using the same water source as the FerryBox (Karlson et al., 2016)~~ Although the analytical precision and accuracy between the two methods seem to be good, the representativeness of both methods may be biased by turbulent wakes, as the validation was carried out within the ~~, which would still be part of the~~ shipping lane ~~area, and not the unaffected waters outside the ship lane~~. Considering the general uncertainty of e.g. seawater temperature measurements being in the order of 0.0025K (e.g. Schmidt 2016), ~~As~~ the measured temperature differences, up to 1°C, between inside and outside the thermal wakes, ~~was up to 1°C in some of the scenes (see Fig. 4 for example)~~(e.g. Fig. 4~~–~~), could increase the uncertainty of the temperature measurements in the FerryBox data significantly. Further,~~and~~ as the bubbly wake affects gas exchange and saturation, it is important to know if the measurements are affected by ship-induced turbulence. Hence, the effect of ship-induced vertical mixing should be considered when using data collected from FerryBox systems.

~~Among the ADCP measurements, there were a few wakes which reached depths of >18 m (Table 2). The deepest wake, >30 m, observed in this dataset was induced by a cargo ship with a beam of 25 m, length of 229 m, and draught of 7 m. It The ship passed the instrument at a distance of 34 m and a speed of 19 knots. The cargo ship had a Gross Tonnage similar to the average of container and Ro-Ro cargo ships in the Baltic Sea (HELCOM, 2018), indicating that ship-induced mixing to depths of 30 m could be a common, but undetected occurrence. The hypothesis that vertical mixing of to this depth could be more frequent than expected from previous studies (Table 2) is supported by the fact observations that similarly sized ships passing at the same distance as the cargo ship inducing the deepest wake, also induced mixing to depths greater than 15 15 m. The lack of previous reports of vertical mixing of this magnitude can partly be explained by the fact that no previous study has targeted this specific research question. Moreover, measurements made using similar methods, but for other purposes, are seldom conducted in ship lanes and particularly not from below. On the other hand, the difference in wake depth for ships of similar~~

size and passing distance could also be due to differences in stratification, as a strong stratification can dampen the vertical development of the wake (Kato and Phillips, 1969). During the ADCP measurement campaign, water column stratification was measured at deployment and retrieval of the instrument (Fig. 4). Three hours before the instrument retrieval, a cargo ship passed at a distance of 21 m and induced a bubble wake of 13.5 m depth and a ~~c~~wake 17.5 m depth. At the point of retrieval, the CTD measurement showed a strong thermal stratification at 5 m depth. At the time of ship passage, intense vertical mixing induced the wake down to 17.5 m depth, and the likelihood that the thermal stratification at 5 m depth was present intact during the longevity of the wake, is small. This means that the stratification was strongly influenced by the wake and that waters above and below the thermocline were mixed with each other. Three hours later the water had re-stratified and the mixed water has had spread out laterally, but t. However, during the longevity of the wake, the stratification was most likely strongly affected, and mixing between water masses would occur. The effect of the mixing, in terms of changes of the physical and chemical characteristics of the water mass, is irreversible. However, the effects of the mixing event that remain after re-stratification (i.e. changes in chemical composition, gas exchange, temperature), are not possible to observe with the methods used in this study. Still, ship-induced turbulence affects the local and regional stratification, even though the contribution from each single ship is difficult to observe with an ADCP after the water has re-stratified. The lack of previous reports of vertical mixing of this magnitude can partly be explained by the fact that no previous study has targeted this specific research question. Moreover, measurements made using similar methods, but for other purposes, are seldom conducted in ship lanes and particularly not from below.

Nevertheless, fFurther studies are needed to determine the impact of stratification on the vertical development of the turbulent wake, and how it varies withthe importance of the ship's draught and speed. Thus, tThe results from this study shows that vertical mixing to depths down to 30 m occurs, and possibly at a high frequency, but. However, as the current knowledge about the wake distribution is poor (especially on a vertical scale), and further studies are needed to determine when, and at which what frequency, vertical mixing reaching this depth occurs.

Commented [AN19]: This section has been moved to section 3.1.4, where we present the results of the wake depth.

3.4 Limitations and Future outlook

The measurements in this study indicated resuspension and turbulence at the sea floor at 30 m depths, induced by the Kelvin wake from passing ships. In shallow water regimes the waves of the Kelvin wake give rise to increased current speeds at the sea floor, which can lead to resuspension (Soomere and Kask, 2003; Soomere, 2007), and Tthe measurements in this study also indicated resuspension and turbulence at the sea floor at 30 m depths, induced by the Kelvin wake from passing ships.. These effects were seen at quite large distances from the passing point, which is expected as the Kelvin wake travels along the sea surface and have a larger spatial extent compared to the turbulent wake. The effect and waves of the Kelvin wake are comparable to swells or wind waves, but their temporal extent is much shorter and the wave characteristics (wave period, significant wave hight) can be different from the natural wave regime. In the Baltic Sea, Danielsson et al. (2007) have shown that wind waves are important for sediment resuspension at more than 40 m depth, which is comparable to the results in this study. However, the effect of Kelvin wakes was outside the scope of the current study but has been investigated by (Soomere

and Kask, 2003; Soomere, 2007); Soomere et al. (2009). Nevertheless, tThese observations indicate the importance of including the effect of the Kelvin wake where shallow water regimes apply, when estimating the environmental impact on the marine environment in intensely trafficked ship lanes. However, the effect of Kelvin wakes is outside the scope of the current study, but has been investigated by Soomere (2007) Soomere et al. (2009).

The lack of detectable thermal wakes in the satellite dataset during the winter months was expected; to entrain cooler water from below, induced by the turbulent wake, and cause a surface temperature gradient, a. A thermal stratification is needed to entrain cooler water from below, induced by the turbulent wake and cause a surface temperature gradient. The Bornholm region usually has a no thermal stratification during winter (Reissmann et al., 2009; van der Lee and Umlauf, 2011). Therefore, the method of estimating the spatiotemporal scales of the turbulent wake using satellite SST measurements is limited to seasons and regions where strong thermal stratifications occur. Moreover, the low percentage of available satellite scenes without too much cloud coverage, little enough cloud cover makes alternative remote sensing techniques, such as drones, a possible alternative. Drones could also be used for a longer time periods in the same area and in combination with under water measurements.

When comparing the observations from the satellite data and the ADCP measurements, remember that they were obtained in different ocean basins and during different stratification conditions. As stated in the methods section, the sites were chosen based on the needs for the two types of measurements. The frequent ship traffic and a separation zone in the Bornholm ship lane made it suitable for detecting the longevity and occurrence of thermal wakes. However, the intense maritime activity in the area and the larger depth, made it both riskier and logistically difficult to place ADCP instruments in the Bornholm ship lane. The authors have previously lost two instruments in the Bornholm area, due to maritime activity, which is why it was considered unsuitable for a longer measurement period. Instead, the Gothenburg area was chosen, as it has a varied and intense ship traffic, with several ferries and cargo vessels on route, ensuring daily passages. It also gave the possibility to access detailed draught information from the ships from the Port of Gothenburg, for the ships visiting the port. The Gothenburg site was not considered suitable for the satellite study, due to the lower amount of ship passages per day and cloudier weather conditions. These circumstances resulted in the decision to use different locations for the two studies. Nevertheless, satellite images were retrieved for the Gothenburg site for the *in situ* measurement period, but they were too cloudy to be usable for any analysis. For future studies focused on characterising the development of the turbulent wake, the ideal would be to make remote sensing and ADCP measurements simultaneously at the same site. However, it would probably be more suitable to use drones instead of satellite images, as a drone is more flexible and makes it possible to operate during cloudy conditions, to capture the development in time, and to use both static and dynamic approaches when documenting the wake.

In addition to the difference in geographical area, the satellite observations show a snapshot of the ocean surface, whereas the ADCP instrument does not measure the top 4 m of the water column. Hence, the two methods never capture the same part of

~~the wake, which could lead to different results using the two methods. Moreover, the satellite observations show the effect of mixing, while ADCP observations show the actual turbulence that causes the mixing. After the mixing has occurred, the mixed water may move outwards – a movement not causing enough turbulence to be seen by the ADCP. This could be one explanation to why the thermal wake longevity is longer, compared to the ADCP wake longevity. Furthermore, the thermal wake being a proxy for the effect of the mixing and not the turbulence itself, is also one of the reasons to why the ADCP results have not been used to estimate a thermal wake depth. However, the large variation in vertical and horizontal distribution of the turbulent wakes observed during the wake analysis (inferred by comparing the signal between the slanted ADCP beams), strongly indicate that the vertical cross section across the width of the turbulent wake is non-uniform and varying. Based on these observations, the vertical cross section of the thermal wake is most likely also non-uniform and will differ in dept along the cross section. However, there is a need for further studies to clarify how the ship design, speed, and propeller (number and rotational direction), interact with water column stratification and currents, in forming the "shape" of the turbulent wake.~~

The ADCP and satellite observations were used to capture different aspects of the turbulent wake, in order to estimate the entire spatiotemporal extent of the turbulent wake. As the thermal wakes show the effect of mixing, while ADCP observations show the actual turbulence that causes the mixing, the two approaches provide different, but complementary results. The difference between the two methods, together with the separate geographical location, limits the possibilities of direct comparison and inference between the results. The observed longevity, for example, was expected to differ between the two approaches, as the turbulence will die out before the effect of the mixing of the water column have disappeared (thermal wake). For wake width, ~~T~~the satellite analysis showed a median wake width of 157.5 m (Fig. 10), implying~~from which it would be expected to~~ that frequent~~ly~~ detection of wakes from ships passing up to 75 m from the instrument, would be expected. This wake width is within the range reported in previous studies (Table 2). The ADCP ~~results indicate a similar range for~~ frequently detected~~ion~~ wakes from ships passing within 0–3 ship widths form the instrument (median of 29 m), indicating slightly narrower wake widths, although distances up to 82 m were present within the close wake subset. ~~A quantitative estimate of the thermal wake depth based on the ADCP results have not been made. However,~~ The large variation in vertical and horizontal distribution of the turbulent wakes observed during the wake analysis (inferred by comparing the signal between the slanted ADCP beams), strongly indicate that the vertical cross section across the width of the turbulent wake is non-uniform and varying. Based on these observations, the vertical cross section of the thermal wake is most likely also non-uniform and will differ in dept along the cross section~~namely 50 m~~. There is a need for further studies to clarify how the ship design, speed, and propeller (number and rotational direction), interact with water column stratification and currents, in forming the "shape" of the turbulent wake.

The lack of detectable thermal wakes in the satellite dataset during the winter months was expected; for ship-induced turbulence to entrain cooler water from below~~, induced by the turbulent wake,~~ and cause a surface temperature gradient, a thermal stratification is needed. The Bornholm region usually has a no thermal stratification during winter (Reissmann et al.,

2009; van der Lee and Umlauf, 2011). Therefore, the method of estimating the spatiotemporal scales of the thermal wake using satellite SST observations is limited to seasons and regions where strong thermal stratifications occur. Moreover, the low percentage of available satellite scenes without too much cloud coverage, makes alternative remote sensing techniques, such as drones, a possible alternative. Drones could also be used for longer time periods in the same area and in combination with under water measurements.

~~When discussing the detection range of the ADCP instrument, the influence of currents and wind should be considered.~~ As a current can move the wake towards or away from the instrument, the current speed and direction must be taken into consideration when estimating at what distance from the ship a wake is likely to be detected. ~~In this study, the water speed and waves were measured with the ADCP, and the wind effect on currents and waves were considered captured by those measurements. As a current can move the wake towards or away from the instrument, the current speed and direction must be taken into consideration when estimating at what distance from the ship a wake is likely to be detected.~~ Trevorrow et al (1994) conducted measurements within 2–5 m of the turbulent wake and reported difficulties in catching the bubble signal from the wake using vertical sonars, as the wake often drifted out of the sonar range before it had completely dissipated. In this study, the water speed and waves were measured with the ADCP, and the wind effect on currents and waves were considered captured by those measurements.~~In this study,~~ ~~A~~a majority of the observed passages (50–60 %) occurred when there was a weak or no current at the position of the ADCP instrument (data not shown). Moreover, a current speed towards the instrument did not increase the likelihood of detecting the wake, especially not when ships passed further away from the instrument (data not shown).~~The difference in temporal longevity, between the ADCP measurements and satellite observations, can partly be explained by the fact that the two methods measures different aspects of the turbulent wake.In addition to the difference in geographical area, the satellite observations show a snapshot of the ocean surface, whereas the ADCP instrument does not measure the top 4 m of the water column. Hence, the two methods never capture the same part of the wake, which could lead to different results using the two methods. Moreover, the satellite observations show the effect of mixing, while ADCP observations show the actual turbulence that causes the mixing.~~

~~After the mixing has occurred, the mixed water may move outwards – a movement not causing enough turbulence to be seen by the ADCP. This could be one explanation to why the thermal wake longevity is longer, compared to the ADCP wake longevity. Furthermore, the thermal wake being a proxy for the effect of the mixing and not the turbulence itself, is also one of the reasons to why the ADCP results have not been used to estimate a thermal wake depth. However, the large variation in vertical and horizontal distribution of the turbulent wakes observed during the wake analysis (inferred by comparing the signal between the slanted ADCP beams), strongly indicate that the vertical cross section across the width of the turbulent wake is non-uniform and varying. Based on these observations, the vertical cross section of the thermal wake is most likely also non-uniform and will differ in dept along the cross section. However, there is a need for further studies to clarify how the ship design, speed, and propeller (number and rotational direction), interact with water column stratification and currents, in forming the "shape" of the turbulent wake.~~

~~In addition to the currents, the width and size of the ship should also be taken into consideration when discussing detection related to the passage distance from the instrument. The distance between the ADCP instrument and ship, is calculated from the position of the AIS transmitter. As the transmitter is often located at the middle of the ship and, a wide ship might be passing right over the instrument even though the AIS stamp indicates that the ship is 25 m away. Thus, larger ships are possibly closer to the instrument than what is registered by the AIS, which could potentially influence the wake detection. To adjust for this bias, the graphical presentation of the data has the distance to the instrument has presented in ship widths instead of meters. A large majority of the ships inducing wakes in the ADCP measurements were 20 m or wider, and the wider ships were overrepresented among the passages inducing wakes, comparing the wake width for the entire dataset. Moreover, the smallest ships (width < 10 m) rarely induced wakes, and then only when passing within 75 m of the ADCP. A similar pattern can also be seen when looking at the length of the ships inducing the wakes.~~

In the current study, the water column stratification was only measured at deployment and retrieval of the instrument, hence the importance of stratification could not be ~~included~~ addressed in ~~the analysis of~~ this study. However, the presence and strength of the stratification will influence how much turbulence that is required to mix water and substances across the thermocline (e.g. Kato and Phillips (1969)). In a stratified fluid, vertical mixing removes energy from the turbulence, reducing the vertical extent of the wake development. Stratification will also cause mixed fluid to spread out laterally, which causes an adjustment of the wake stratification to the surrounding stratification, resulting in a widening of the wake as well as an additional limitation of the vertical extent (Voropayev et al., 2012). As the aim of the current study was to present an order of magnitude estimation of the spatial and temporal scales of the turbulent wake, the lack of stratification measurements does not present an immediate ~~at~~ problem within the current scope, yet it could be one explanation for the absence of statistically significant correlations between wake depth and vessel force. ~~However, f~~For future studies ~~with the aim of~~aiming at characterising the development of the turbulent wake and quantifying the ship-induced vertical mixing, stratification measurements will be necessary in order to understand the interaction between the stratification and the turbulent wake. ~~Moreover, as the stratification must be expected to be an important factor for wake depth, it could be one explanation for the absence of statistically significant correlations between wake depth and vessel force.~~

In shallow water regimes the waves of the Kelvin wake give rise to increased current speeds at the sea floor, which can lead to resuspension (Soomere and Kask, 2003; Soomere, 2007). ~~and~~The measurements in this study also indicated resuspension and turbulence at the sea floor at 30 m depths, induced by the Kelvin wake from passing ships. These observations indicate the importance of including the effect of the Kelvin wake where shallow water regimes apply, when estimating the environmental impact on the marine environment in intensely trafficked ship lanes. However, the effect of Kelvin wakes is

outside the scope of the current study, but has been investigated by Soomere and Kask (2003), Soomere (2007), and Soomere et al. (2009).

Finally, ~~I~~in order to determine when vertical mixing reaching depths of 30 m occurs, and how common it is, future studies need to simultaneously measure the wake in more than one point, ~~in order~~ to ~~get~~ capture the 2D cross section, i.e. both the depth and the width of the wake. One way of achieving this would be to conduct measurements with several ADCPs placed on a row perpendicular to the ship lane. ~~This would give a cross-section of the wake, which could be used to describe both the width and depth of the turbulent wake. As the measurements in this study were made using one instrument, only the depth of the wake could be measured, and only at one point in the wake cross-section.~~ Moreover, a line of instruments would also be able to capture a drifting wake and thus better estimate the true longevity. One of the limitations of the longevity estimation in this study, is that currents could potentially shift the wake away from the instrument. Using multiple instruments would increase the chance of capturing the entire wake development, as it would cover a larger area, thus increasing the reliability of the longevity estimation. As the results from this study indicate that proximity is of importance for detecting the turbulent wakes using ADCP measurements, multiple instruments would increase the area where ships can pass close to the instrument. In addition, if the maximum depth of the wake is located only in a certain region of the turbulent wake, the likelihood of measuring that part of the wake is small when only one instrument is used. This spatial limitation of the current study makes it difficult to determine if the small number of detected deep wakes was because of low occurrence, or because using only one instrument made it difficult to successfully ~~measure~~ capture the deepest part of the wake. Thus, multiple instruments would increase the ability to identify when and where the very deep mixing occurs and shed further light upon how frequently deep mixing is induced. Conducting concurrent measurements using ADCPs and remote sensing, ~~It~~ would also be beneficial ~~to conduct concurrent measurements using ADCPs and remote sensing~~. In the current study, the satellite analysis and ADCP measurements have been conducted at different locations and time periods, but concurrent measurements would be necessary for obtaining a more complete picture of the how the three-dimensional wakes develop for various combinations of stratification, vessel dimensions, propeller properties, and vessel speed. ~~give a more complete picture of both the large horizontal temporal and spatial scales, as well as the vertical scales.~~

4 Conclusions

Based on a large sample of *in situ* measurements, the median spatiotemporal extent of turbulent ship wakes ~~have~~ has been estimated to a depth of 13.5 m and longevity of 09:59 min, based on ADCP measurements. Thermal wake width and longevity have been estimated to a median of 157.5 m and 13.7 km respectively, based on SST satellite image analysis. The results show frequent detection of turbulent wakes deeper than 12 m, which is deeper than previously reported. Moreover, in areas with intense ship traffic, the presented temporal and spatial extent of the turbulent wakes are of a scale relevant to consider when assessing environmental impact from shipping.

5 Data Availability

Acoustic measurement data available upon request for non-commercial purposes. AIS data available through HELCOM according to their data policy. Satellite images freely available at https://s3-us-west-2.amazonaws.com.

6 Author contribution

I-M. Hassellöv, A. T. Nylund, L. Arneborg and A. Tengberg conceptualised and conducted the *in situ* field measurements and consecutive analysis and visualisation. A. T. Nylund developed the code used in the analysis, with contribution from L. Arneborg. U. Mallast conducted the data curation and formal analysis of the satellite images, with contribution from A. T. Nylund. The manuscript was prepared by A. T. Nylund with contributions from all co-authors.

7 Competing interests

The authors declare that they have no conflict of interest.

8 Acknowledgements

Acknowledgment of funding for the OCEANSensor project by the Research Council of Norway (project number 284628) and co-funding by the European Union 2020 Research and Innovation Program, as part of the MarTERA Program. Acknowledgement to the Swedish Institute for the Marine Environment (SIME), for supplying the AIS dataset. This work has been partially supported by MarineTraffic, by the use of their database of vessel information.

9 Abbreviations

ADCP - Acoustic Doppler Current Profiler
AIS - Automatic Information System
ANOVA - Analysis of Variance
EOF - Empirical Orthogonal Function
HELCOM - Baltic Marine Environment Protection Commission
IMO - International Maritime Organization
MCR - Maximum Continuous Rating
MNDWI - modified normalized difference water index
NDRC - National Defense Research Committee
SIME - Swedish Institute for the Marine Environment

SMHI - Swedish Meteorological and Hydrological Institute

TIRS - Thermal Infrared Sensor

TOA - top-of-the-atmosphere

References

Andersson, L., and Rydberg, L.: Exchange of water and nutrients between the Skagerrak and the Kattegat, Estuar. Coast. Shelf Sci., 36, 159-181, 1993.

Arneborg, L.: Mixing efficiencies in patchy turbulence, J. Phys. Oceanogr., 32, 1496-1506, 2002.

Balcombe, P., Brierley, J., Lewis, C., Skatvedt, L., Speirs, J., Hawkes, A., and Staffell, I.: How to decarbonise international shipping: Options for fuels, technologies and policies, Energ. Convers. Manage., 182, 72-88, https://doi.org/10.1016/j.enconman.2018.12.080, 2019.

Barsi, J. A., Barker, J. L., and Schott, J. R.: An Atmospheric Correction Parameter Calculator for a single thermal band earth-sensing instrument, IGARSS 2003. 2003 IEEE International Geoscience and Remote Sensing Symposium. Proceedings (IEEE Cat. No.03CH37477), Centre de Congress Pierre Bandis, Toulouse, France 21-25 July, 2003.

Bickel, S. L., Malloy Hammond, J. D., and Tang, K. W.: Boat-generated turbulence as a potential source of mortality among copepods, J. Exp. Mar. Biol. Ecol., 401, 105-109, https://doi.org/10.1016/j.jembe.2011.02.038, 2011.

Buhaug, Ø., Corbett, J., Endresen, Ø., Eyring, V., Faber, J., Hanayama, S., Lee, D. S., Lee, D., Lindstad, H., Markowska, A. Z., Mjelde, A., Nelissen, D., Nilsen, J., Pålsson, C., Winebrake, J., Wu, W., and Yoshida, K.: Second IMO GHG study 2009, International Maritime Organisation (IMO), London, 2009.

Carrica, P. M., Drew, D., Bonetto, F., and Lahey, R. T.: A polydisperse model for bubbly two-phase flow around a surface ship, Int. J. Multiphase Flow, 25, 257-305, https://doi.org/10.1016/S0301-9322(98)00047-0, 1999.

Danielsson, Å., Jönsson, A., and Rahm, L.: Resuspension patterns in the Baltic proper, J. Sea Res., 57, 257-269, 2007.

Emerson, S., and Bushinsky, S.: The role of bubbles during air-sea gas exchange, J. Geophys. Res.-Oceans, 121, 4360-4376, https://doi.org/10.1002/2016jc011744 2016.

Ermakov, S. A., and Kapustin, I. A.: Experimental study of turbulent-wake expansion from a surface ship, Izv. Atmos. Ocean. Phy+, 46, 524-529, https://doi.org/10.1134/S0001433810040110, 2010.

Foga, S., Scaramuzza, P. L., Guo, S., Zhu, Z., Dilley, R. D., Beckmann, T., Schmidt, G. L., Dwyer, J. L., Joseph Hughes, M., and Laue, B.: Cloud detection algorithm comparison and validation for operational Landsat data products, Remote Sens. Environ., 194, 379-390, https://doi.org/10.1016/j.rse.2017.03.026, 2017.

Francisco, F., Carpman, N., Dolguntseva, I., and Sundberg, J.: Use of Multibeam and Dual-Beam Sonar Systems to Observe Cavitating Flow Produced by Ferryboats: In a Marine Renewable Energy Perspective, J. Mar. Sci. Eng., 5, 30, https://doi.org/10.3390/jmse5030030, 2017.

Fu, H., and Wan, P.: Numerical simulation on ship bubbly wake, Journal of Marine Science and Application, 10, 413-418, https://doi.org/10.1007/s11804-011-1086-x, 2011.

Fujimura, A., Soloviev, A., Rhee, S. H., and Romeiser, R.: Coupled Model Simulation of Wind Stress Effect on Far Wakes of Ships in SAR Images, IEEE T. Geosci. Remote, 54, 2543-2551, https://doi.org/10.1109/TGRS.2015.2502940, 2016.

Garrison, H. S., and Tang, K. W.: Effects of episodic turbulence on diatom mortality and physiology, with a protocol for the use of Evans Blue stain for live–dead determinations, Hydrobiologia, 738, 155-170, 10.1007/s10750-014-1927-0, 2014.

Gilman, M., Soloviev, A., and Graber, H.: Study of the far wake of a large ship, J. Atmos. Ocean. Tech., 28, 720-733, https://doi.org/10.1175/2010JTECHO791.1, 2011.

Golbraikh, E., and Beegle-Krause, C.: A model for the estimation of the mixing zone behind large sea vessels, Environmental Science and Pollution Research, 27, 37911-37919, 2020.

Hassellöv, I., Larsson, K., and Sundblad, E.: Effekter på havsmiljön av att flytta över godstransporter från vägtrafik till sjöfart. Rapport nr 2019:5, Havsmiljöinstitutet, 2019.

Heiselberg, H.: A direct and fast methodology for ship recognition in Sentinel-2 multispectral imagery, Remote Sens., 8, 1033, https://doi.org/10.3390/rs8121033, 2016.

HELCOM: Maritime Activities in the Baltic Sea—An Integrated Thematic Assessment on Maritime Activities and Response to Pollution at Sea in the Baltic Sea Region, Balt. Sea Environ. Proc. No. 123, Helsinki Commission (HELCOM), Helsinki, Finland, 65, 2010.
HELCOM: HELCOM Assessment on maritime activities in the Baltic Sea 2018. Baltic Sea Environment Proceedings No.152, Helsinki Commission, Helsinki, Finland, 253, 2018.
Issa, V., and Daya, Z. A.: Modeling the turbulent trailing ship wake in the infrared, Appl. Opt., 53, 4282-4296, https://doi.org/10.1364/AO.53.004282, 2014.
Jakobsson, M., Stranne, C., O'Regan, M., Greenwood, S. L., Gustafsson, B., Humborg, C., and Weidner, E.: Bathymetric properties of the Baltic Sea, Ocean Sci., 15, 905-924, 10.5194/os-15-905-2019, 2019.
Jalkanen, J.-P., Johansson, L., and Kukkonen, J.: A Comprehensive Inventory of the Ship Traffic Exhaust Emissions in the Baltic Sea from 2006 to 2009, Ambio, 43, 311-324, 10.1007/s13280-013-0389-3, 2014.
Karlson, B., Andersson, L., Kaitala, S., Kronsell, J., Mohlin, M., Seppälä, J., and Wranne, A. W.: A comparison of Ferrybox data vs. monitoring data from research vessels for near surface waters of the Baltic Sea and the Kattegat, J. Mar. Syst., 162, 98-111, doi: 10.1016/j.jmarsys.2016.05.002, 2016.
Kato, H., and Phillips, O.: On the penetration of a turbulent layer into stratified fluid, J. Fluid Mech., 37, 643-655, doi: 10.1017/S0022112069000784, 1969.
Katz, C. N., Chadwick, D. B., Rohr, J., Hyman, M., and Ondercin, D.: Field measurements and modeling of dilution in the wake of a US navy frigate, Mar. Pollut. Bull., 46, 991-1005, https://doi.org/10.1016/S0025-326X(03)00117-6, 2003.
Leppäranta, M., and Myrberg, K.: Physical oceanography of the Baltic Sea, Springer Science & Business Media, 2009.
Liefvendahl, M., and Wikström, N.: Modelling and simulation of surface ship wake signatures, Report FOI-R--4344--SE, Swedish Defence Research Agency (FOI), Stockholm, 36, 2016.
Loehr, L., Mearns, A., and George, K.: Initial report on the 10 July 2011 study of opportunity: currents and wake turbulence behind cruise ships, Alaska Department of Environmental Quality, 2001.
Loehr, L. C., Beegle-Krause, C.-J., George, K., McGee, C. D., Mearns, A. J., and Atkinson, M. J.: The significance of dilution in evaluating possible impacts of wastewater discharges from large cruise ships, Mar. Pollut. Bull., 52, 681-688, https://doi.org/10.1016/j.marpolbul.2005.10.021, 2006.
Lucas, N., Simpson, J., Rippeth, T., and Old, C.: Measuring turbulent dissipation using a tethered ADCP, J. Atmos. Ocean. Tech., 31, 1826-1837, https://doi.org/10.1175/JTECH-D-13-00198.1, 2014.
Mallast, U., and Siebert, C.: Combining continuous spatial and temporal scales for SGD investigations using UAV-based thermal infrared measurements, Hydrology & Earth System Sciences, 23, 2019.
Marmorino, G., and Trump, C.: Preliminary side-scan ADCP measurements across a ship's wake, J. Atmos. Ocean. Tech., 13, 507-513, https://doi.org/10.1175/1520-0426(1996)013<0507:PSSAMA>2.0.CO;2, 1996.
Moldanová, J., Fridell, E., Matthias, V., Hassellöv, I.-M., Eriksson, M., Jalkanen, J.-P., Tröeltzsch, J., Quante, M., Johansson, L., and Majutenko, I.: Information on completed BONUS SHEBA project, Baltic Marine Environment Protection Commission, Maritime Working Group, MARITIME 18-2018, Hamburg, Germany, 18, 2018.
NDRC: The Physics of Sound in the Sea, United States Office of Scientific Research and Development, National Defense Research Committee, Division 6, Washington, D.C., 1946.
Otsu, N.: A Threshold Selection Method from Gray-Level Histograms, IEEE T. Syst. Man Cyb., 9, 62-66, https://doi.org/10.1109/TSMC.1979.4310076, 1979.
Parmhed, O., and Svennberg, U.: Simulering av luftbubblor och ytvågor runt ytfartyg, Repot FOI-R-2217-SE, FOI - Swedish Defence Research Agency, Tumba, 2006.
Petersen, W.: FerryBox systems: State-of-the-art in Europe and future development, J. Mar. Syst., 140, 4-12, doi: 10.1016/j.jmarsys.2014.07.003, 2014.
Reissmann, J. H., Burchard, H., Feistel, R., Hagen, E., Lass, H. U., Mohrholz, V., Nausch, G., Umlauf, L., and Wieczorek, G.: Vertical mixing in the Baltic Sea and consequences for eutrophication–A review, Prog. Oceanogr., 82, 47-80, https://doi.org/10.1016/j.pocean.2007.10.004, 2009.
Smirnov, A., Celik, I., and Shi, S.: LES of bubble dynamics in wake flows, Comput. Fluids, 34, 351-373, https://doi.org/10.1016/j.compfluid.2004.05.004, 2005.
Smith, S. D.: Coefficients for sea surface wind stress, heat flux, and wind profiles as a function of wind speed and temperature, Journal of Geophysical Research: Oceans, 93, 15467-15472, 1988.

Smith, T. W., Jalkanen, J., Anderson, B., Corbett, J., Faber, J., Hanayama, S., O'keeffe, E., Parker, S., Johanasson, L., and Aldous, L.: Third IMO GHG study 2014, International Maritime Organisation (IMO), London, 2015.
Snoeijs-Leijonmalm, P., and Andrén, E.: Biological oceanography of the Baltic Sea, Springer Science & Business Media, Dordrecht, Netherlands, 683 pp., 2017.
Soloviev, A., Gilman, M., Young, K., Brusch, S., and Lehner, S.: Sonar measurements in ship wakes simultaneous with TerraSAR-X overpasses, IEEE T. Geosci. Remote, 48, 841-851, https://doi.org/10.1109/TGRS.2009.2032053, 2010.
Soloviev, A., Maingot, C., Agor, M., Nash, L., and Dixon, K.: 3D sonar measurements in wakes of ships of opportunity, J. Atmos. Ocean. Tech., 29, 880-886, https://doi.org/10.1175/JTECH-D-11-00120.1, 2012.
Soomere, T., and Kask, J.: A specific impact of waves of fast ferries on sediment transport processes of Tallinn Bay, Proc. Estonian Acad. Sci. Biol. Ecol, 52, 319-331, 2003.
Soomere, T.: Nonlinear Components of Ship Wake Waves, ApMRv, 60, 120-138, 10.1115/1.2730847, 2007.
Soomere, T., Parnell, K., and Didenkulova, I.: Implications of fast-ferry wakes for semi-sheltered beaches: a case study at Aegna Island, Baltic Sea, J. Coast. Res., 128-132, 2009.
Stanic, S., Caruthers, J. W., Goodman, R. R., Kennedy, E., and Brown, R. A.: Attenuation measurements across surface-ship wakes and computed bubble distributions and void fractions, IEEE J. Oceanic Eng., 34, 83-92, https://doi.org/10.1109/JOE.2008.2008411, 2009.
Stigebrandt, A.: Physical oceanography of the Baltic Sea, in: A systems analysis of the Baltic Sea, Springer, 19-74, 2001.
Sutherland, P., and Melville, W. K.: Field measurements of surface and near-surface turbulence in the presence of breaking waves, J. Phys. Oceanogr., 45, 943-965, 2015.
Swedish Maritime Administration, Nautical Information - Sjofartsverket: https://www.sjofartsverket.se/en/Maritime-services/Pilotage/Pilot-Areas/Goteborg-Pilot-Area/Harbour-Information-Goteborg/, access: 18 May 2020, 2020.
The Port of Gothenburg: https://www.portofgothenburg.com/FileDownload/?contentReferenceID=12900, access: May 18, 2020.
Thorpe, S. A.: An introduction to ocean turbulence, Cambridge University Press, New York, 240 pp., 2007.
Trevorrow, M. V., Vagle, S., and Farmer, D. M.: Acoustical measurements of microbubbles within ship wakes, J. Acoust. Soc. Am., 95, 1922-1930, https://doi.org/10.1121/1.408706, 1994.
UNCTAD: Review of Maritime Transport 2019, UNCTAD/RMT/2019, United Nations Publications, New York, 2019.
US-EPA: Cruise Ship Plume Tracking Survey Report, U.S. Environmental Protection Agency, Washington, D.C, 2002.
van der Lee, E. M., and Umlauf, L.: Internal wave mixing in the Baltic Sea: Near-inertial waves in the absence of tides, JGRC, 116, doi: 10.1029/2011jc007072, 2011.
Vollmer, M.: Newton's law of cooling revisited, EJPh, 30, 1063, 2009.
Voropayev, S., Nath, C., and Fernando, H.: Thermal surface signatures of ship propeller wakes in stratified waters, Phys. Fluids, 24, 116603, https://doi.org/10.1063/1.4767130, 2012.
Weber, T. C., Lyons, A. P., and Bradley, D. L.: An estimate of the gas transfer rate from oceanic bubbles derived from multibeam sonar observations of a ship wake, JGRC, 110, https://doi.org/10.1029/2004JC002666, 2005.
Xu, H.: Modification of normalised difference water index (NDWI) to enhance open water features in remotely sensed imagery, Int. J. Remote Sens., 27, 3025-3033, https://doi.org/10.1080/01431160600589179, 2006.